Spring 2015

Model predictive current control of switched reluctance motor with inductance auto-calibration

Xin Li

Department:

MODEL PREDICTIVE CURRENT CONTROL OF SWITCHED RELUCTANCE MOTOR WITH INDUCTANCE AUTO-CALIBRATION

by

Xin Li

A THESIS

Presented to the Faculty of the Graduate School of the

MISSOURI UNIVERSITY OF SCIENCE AND TECHNOLOGY

In Partial Fulfillment of the Requirements for the Degree

MASTER OF SCIENCE IN ELECTRICAL ENGINEERING

2015

Approved by

Dr. Pourya Shamsi, Advisor
Dr. Mehdi Ferdowsi
Dr. Jonathan W. Kimball

PUBLICATION THESIS OPTION

This thesis has been prepared in publication format. Pages 1-3 have been added to supply background information for the remainder of the thesis. Paper I, pages 4-17, is entitled "Adaptive Model Predictive Control For DSSRM Drives", and is prepared in the style used by the Institute of Electrical and Electronics Engineers (IEEE) Transportation Electrification Conference as published in June 2014. Paper II, pages 18-39, is entitled "Model Predictive Current Control Of Switched Reluctance Motors With Inductance Auto-Calibration", and is prepared in the style used by the IEEE Transactions on Industrial Electronics as submitted on March 31, 2015. Paper III, pages 40-62, is entitled "Inductance Surface Learning For Model Predictive Current Control Of Switched Reluctance Motors", and is prepared in the style used by IEEE Transactions on Transportation Electrification and as submitted on April 1, 2015.

ABSTRACT

The thesis is composed of three papers, which investigate the application of Model Predictive Controller (MPC) for current control of Switched Reluctance Motor (SRM). Since the conventional hysteresis current control method is not suitable for high power SRM drive system with low inductance and limited switching frequency, MPC is a promising alternative approach for this application. The proposed MPC can cope with the measurement noise as well as uncertainties within the machine inductance profile. In the first paper, a MPC current control method for Double-Stator Switched Reluctance Motor (DSSRM) drives is presented. A direct adaptive estimator is incorporated to follow the inductance variations in a DSSRM. In the second paper, the Linear Quadratic (LQ) form and dynamic programming recursion for MPC are analyzed, afterwards the unconstrained MPC solution for stochastic SRM model is derived. The Kalman filter is employed to reduce the variance of measurement noises. Based on Recursive Linear-Square (RLS) estimation, the inductance profile is calibrated dynamically. In the third paper, a simplified recursive MPC current control algorithm for SRM is applied for embedded implementation. A novel auto-calibration method for inductance surface estimation is developed to improve current control performance of SRM drive in statistic terms.

ACKNOWLEDGMENTS

First of all, I would like to express my deep gratitude to my advisor Dr. Pourya Shamsi. Without his patience, guidance, and support, my Master program won't move so smoothly. In addition, his solid theoretical foundation and rich practical experiences help me overcome difficulties in research. My sincere thanks also go to other respectable committee members, Dr. Ferdowsi and Dr. Kimball. I benefit a lot from their insightful teaching, academic seminars, and colloquiums. Moreover, I want to thank all teachers who had taught me in my two year Master program in Missouri University of Science and Technology. Their contribution of time, hard working, and advice to my academic improvement are highly appreciated.

I would also like to thank my colleagues in power lab. Their critical discussion and suggestions push me to explore more on the research. And their friendship and consideration is also a kind of support for me.

Finally, thanks from my bottom of heart go to my family. They constantly love, encourage, and support me without any conditions or reservation. What I had finished and achieved would be impossible without my family.

TABLE OF CONTENTS

LIST OF ILLUSTRATIONS

1. INTRODUCTION

Duo to the ever-developing transportation electrification and climate control technologies in past decade, concerns have been continuously expressed over finding a reliable and economic motor with satisfactory performance. Switched Reluctance Motor (SRM) exhibits many advantages over other type of motors in variable speed system such as the rugged structure due to the magnet free rotor, fault tolerant for lock rotor and stalling, low back Electromotive Force (EMF) for wide speed range. In addition, SRM's relative low material and manufacture cost are considered as attractive characteristic for mess production.

SRMs operate based on complete switching of the phase current within each phase of the motor. Thus, the drive of SRM must cope with nonlinear inductance of windings. Recently, many scholars have explored the current control strategies of SRM. The foci can be categorized to three trends: controller with Pulse Width Modulation (PWM), hysteresis type controller, and non-conventional methods such as neural networks. Among the latest current control technologies in practical terms, Model Predictive Control (MPC) is a promising approach and attracts attention. MPC used to be developed for industrial processing control and successfully applied to power electronics recently. Particularly, MPC can handle the non-linear magnetic characteristic of SRMs, provide fast response, and maintain a fixed switching frequency.

The Finite Control Set MPC (FCS-MPC or Direct MPC) and the general MPC with

PWM are two of main options within scope of research for SRM drive. Although FCS-MPC has been well studied in literatures, it is based on voltage vectors theory and thus can be considered as hysteresis control. In consequence, it is not a appropriate current controller for high power SRM with low inductance and limited switching frequency. The general MPC calculates PWM duty cycle from current feedback, thus it can maintain low current ripple without requirement of high switching frequency. Since the calculation is based on SRM model, having accurate inductances can significantly reduce the current ripples and provide the desired behavior. Another challenge of MPC is the requirement of computation capability. The matrix inverse computation is very time consuming in real-time processing. Hence, effective and precise MPC solving is of interest.

In addition, due to electromagnetic interferences or zero drift the current feedback from sensors contains a significant amount of noise and disturbances. Therefore it is imperative to calibrate MPC inner model and filter current sampling noises under stochastic system.

In order to address above issues, the concept of MPC current control of SRM with auto-calibration is presented. Specifically, three different employment methods are developed and proposed in below three papers, respectively.

In the first paper, a MPC current controller for Double-Stator Switched Reluctance Motor (DSSRM) drives is presented. The inductance variation is estimated and tracked by a direct adaptive estimator which is combined into MPC algorithm. By assuming noise

absence, the proposed adaptive estimator convergence is proved by Lyapunov stability.

In the second paper, the Linear Quadratic (LQ) form and dynamic programming recursion for MPC are analyzed, afterwards the unconstrained MPC solution for stochastic SRM model is derived. The Kalman filter is employed to reduce the variance of current measurement noises. A simplified recursive MPC current control algorithm for SRM is applied for embedded implementation. Based on Recursive Linear-Square (RLS) estimation, the inductance profile in manner of analytic expression is calibrated dynamically.

In the third paper, the MPC current control of SRM is implemented for practical deployments in hybrid vehicle applications. The inductance surface is established by 3-D lookup table, which is quantized for nonlinearity of SRM. The Kalman filter is integrated into MPC. The delay compensation is considered due to the zero-order-hold delay during current sampling. Additionally, a learning mechanism is developed to improve current control performance of SRM drive in statistic terms.

I. ADAPTIVE MODEL PREDICTIVE CONTROL FOR DSSRM DRIVES

Xin Li†, Student Member, IEEE, Pourya Shamsi††, Member, IEEE

Abstract

This paper presents a new current control method for Double-Stator Switched Reluctance Motor (DSSRM) Drives. The proposed current controller is based on Model Predictive Control (MPC) strategy. Moreover, an adaptive estimator is incorporated to follow the inductance variations in a DSSRM. After the introduction of the control method, the proposed controller is validated using simulations. Experimental results will be provided to evaluate the performance improvement.

Index Terms

SRM, MPC, adaptive, predictive control, motor drive, current control.

I. INTRODUCTION

Due to a radical transportation electrification in the past decade, low cost and highly efficient electric motors are of interest. Switched Reluctance Machines (SRM) are good candidates for the future of transportation electrification. SRMs demonstrate high efficiencies and high torque performances while benefitting from low cost of manufacturing. Moreover, due to the inherent simplicity in the magnetic circuit, SRMs are highly reliable. Torque generation in a SRM is based on variations of the magnetic reluctances. Double Stator Switched Reluctance Machines (DSSRM) have demonstrated higher torque densities compared to the conventional SRMs [1]–[3]. This improvement is a result of

† Xin Li is currently a graduate student at Missouri University of Science and Technology, Rolla, Missouri 65409 USA (email: xlg66@mst.edu).

†† Pourya Shamsi is currently with Missouri University of Science and Technology, Rolla, Missouri 65409 USA (email: shamsip@mst.edu).

a superior magnetic structure that increases the aligned to non-aligned reluctance ratio. However, the increased nonlinearities render the conventional current control methods ineffective. On the other hand, in order to achieve higher speed ratio, the average values of inductances in a DSSRM are orders of magnitude lower compared to induction machines. This is to ensure fast rise times at the firing angles as well as low tail currents. Therefore, current regulation in a SRM represent technical challenges. Hence, highly dynamic control methods are required to ensure fast tracking of the reference currents.

Conventionally, hysteresis current control methods have been incorporated to guarantee fast tracking of the reference current in SRM applications. However, in the case of a high power, high speed ratio DSSRM for automotive applications, the phase inductances are small. Therefore, fast switching frequencies are required to maintain an acceptable current ripple in each phase [4]–[6]. On the other hand, in a high power motor drive, the switching frequency is limited by the commercially available semiconductor switches.

Various advanced control approaches have been researched for current control of a SRM. Predictive control methods have been widely used in power electronics applications [7]. MPC has been utilized for control of a SRM [8], [9]. Moreover, adaptive control methods have been utilized to cope with nonlinearities in SRM drives [10]. Adaptive predictive controller has been utilized for high performance control of nonlinear systems [11]–[13].

An adaptive model predictive current control method for DSSRM current control is proposed in this paper. In the first section, a MPC is developed using the model of a DSSRM. This receding horizon control method is designed to eliminate the current error in one switching cycle. Furthermore, in order to cope with the time varying inductances of a DSSRM, Lyapunov adaptive estimator is adopted to follow motor parameters using real-time calculations. Afterwards, simulation and experimental results are provided to demonstrate the effectiveness of the proposed controller.

II. MODEL OF THE DSSRM

This paper studies a 3-phase 8/12 DSSRM. The cross section of this motor is illustrated in Figure 1. The model of a DSSRM is similar to the model of conventional SRMs. Hence, the dynamic equations for one phase of a DSSRM can be expressed as

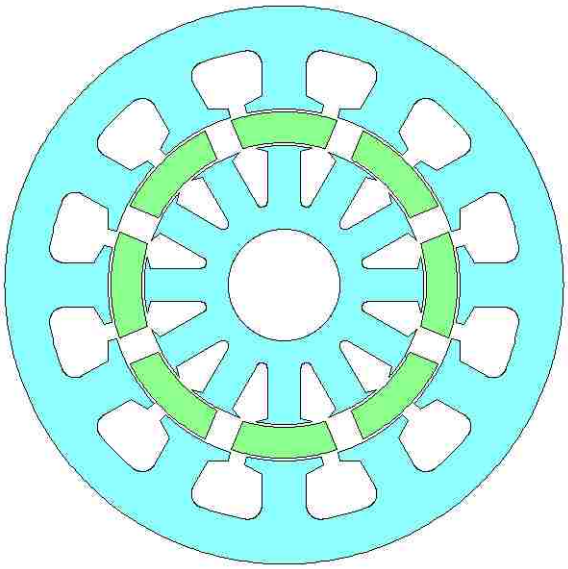

Fig. 1. Cross section of a 8/12 DSSRM.

$$v\left(t\right)=Ri\left(t\right)+\frac{\partial\Psi\left(i\left(t\right),L\left(\theta,i\right)\right)}{\partial t}=Ri\left(t\right)+L\left(\theta,i\right)\frac{di\left(t\right)}{dt}+i\left(t\right)\frac{\partial L\left(\theta,i\right)}{\partial t} \tag{1}$$

where R represents phase resistance which is known and considered as a constant. $\Psi(t)$, $v(t)$, and $i(t)$ are the flux linkage, phase voltage, and phase current, respectively. $L(\theta,i)$ is the inductance of the motor which is nonlinear with respect to the amplitude of the current and the phase angle of the rotor (i.e. θ). Defining the rotor speed as ω, (1) is simplified as

$$v\left(t\right)=i\left(t\right)\left[R+\omega\frac{\partial L\left(\theta,i\right)}{\partial\theta}\right]+L\left(\theta,i\right)\frac{di\left(t\right)}{dt} \tag{2}$$

Moreover, the inductance profile of a SRM can be estimated using Fourier series as [14]

$$L\left(\theta,i\right)=c_0\left(i\right)+c_1\left(i\right)\cos\left(8\theta\right)+c_2\left(i\right)\cos\left(16\theta\right) \tag{3}$$

where

$$4c_0(i)=L_a(i)+2L_m(i)+L_u(i) \tag{4}$$

$$4c_1(i)=-2L_a(i)+2L_u(i) \tag{5}$$

$$4c_2(i)=L_a(i)-2L_m(i)+L_u(i) \tag{6}$$

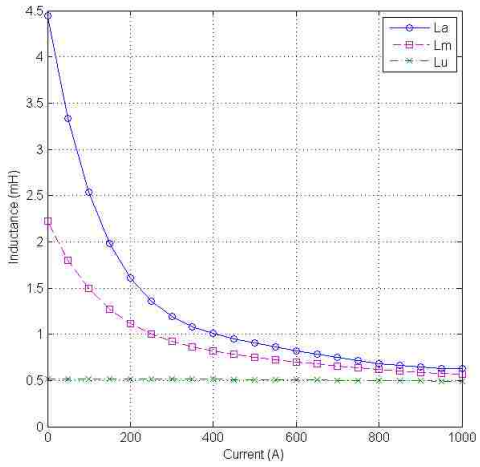

Fig. 2. Variations of the inductance coefficients as a function of the phase current.

and L_a, L_m, and L_u are aligned, mid-point, and unaligned inductances of the motor as shown in Figure 2. In order to optimize the MPC for digital implementation, using z-transform, the model in the discrete-time domain can be derived as

$$I\left(k\right) = \frac{V(k)T_m + V(k-1)T_m}{G(k)} + \frac{I(k-1)\left(4L(\theta, I(k)) - G(k)\right)}{G(k)} \tag{7}$$

where

$$G(k) = 2L(\theta, I(k)) + T_m R + \omega(k) T_m \frac{\partial}{\partial \theta} L(\theta, I(k)) \tag{8}$$

and $I(k)$ and $V(k)$ are current and voltage at the k-th sample time. T_m is the sampling interval (i.e. reciprocal of control frequency). $L(\theta, I(k))$ is the inductance at the $I(k)$. This value is a function of the current and phase angle of the motor. $dL(\theta, I(k))/d\theta$ is the rate of the variations in the inductance with respect to variations of the rotor angle.

III. CONTROLLER DESIGN

A. Model Predictive Current Control

The topology considered for the converter of each phase is shown in Figure 3. The predictive controller gives the switching signals for upper bridge, S_2. The lower switch, S_1, is controlled based on the rotor position and operating mode of the machine. In this case, the winding current is controlled in soft chopping mode by predictive controller

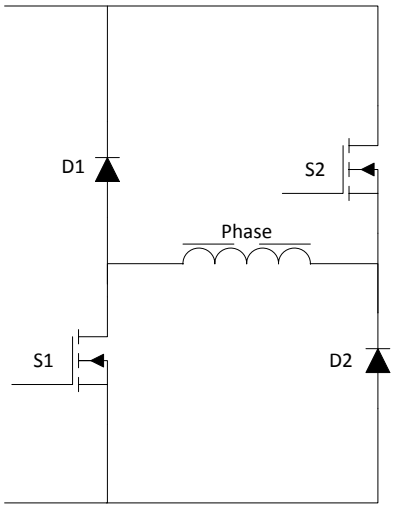

Fig. 3. Converter circuit topology for each phase.

during the conduction band to produce torque. The phase is turned off in hard chopping mode to guarantee a fast negative slope for the current. In general, Model Predictive Control (MPC) of the current of each phase can be calculated using

$$\underset{V(k+1)}{\arg\min}\ J := \sum_{i=1}^{N} c_i (I^{ref} - I(k+i))^2 \tag{9}$$

with no cost for the input and with the constraint of (7). Also, in order to reduce the processing requirements, an assumption of $V(i+1) = V(i)$ is added as a constraint. By increasing the strength of c_N, the voltage of each step can be estimated without a requirement for dynamic optimizations. This can be modeled by reducing the apparent sampling time for the MPC. By considering a sampling time of NT_m, a single step model predictive control is derived with an optimized input of

$$V\,(k+1) \simeq I^{ref}\left[R + \omega(k)\frac{\partial L(\theta, I^{ref})}{\partial \theta}\right] + f_m(I^{ref} - I(k))L(\theta, I(k)) + Vc \tag{10}$$

Where f_m is $1/(T_m N)$ and Vc is to compensate for the voltage drop of the converter. A simplified MPC is applied here to reduce the processing requirements and provide more

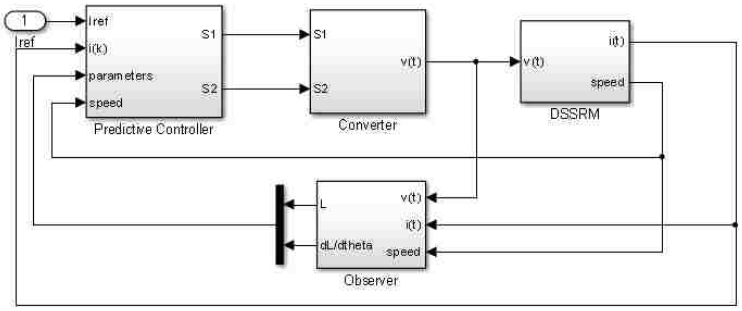

Fig. 4. The proposed control strategy.

immunity to the noise. If a single-step MPC is implemented (i.e. $N = 1$), the derivative term will lead to amplification of the noise. However, by reducing the strength of the derivative with a factor of N, better immunity to the sampling noise is achieved. Hence, if the control objective is to achieve I^{ref}, which is the reference current given from speed loop controller, at the N-th switching period, $V(k + 1)$ is the voltage that needs to be applied to the motor. Therefore, a basis for a model predictive controller is developed.

B. Adaptive Control

The motor inductances are affected by saturation of the magnetic core. Moreover, the accurate dynamical measurement of the phase inductance represent technical challenges. Significant portion of the variations of the model is due to aging of the system, high temperatures, and saturation of the machine. Fortunately, the frequency of these variations are small. It should be noted that the high frequency variations are modeled using the Fourier and Taylor series representation of the sinusoidal inductance profiles and saturation of the coefficients, respectively. However, the actual inductance is different from the calculated inductance using the Taylor and Fourier series. Inductances can be measured in real-time using high frequency current injection into phases of the SRM. However, this method requires high processing power as well as accurate measurements. In this section, an adaptive observer is integrated with the MPC to track the low frequency variations of the model.

Based on

$$\frac{di\,(t)}{dt} = -i\,(t)\,\frac{R + \omega\partial L(\theta, i)/\partial\theta}{L(\theta, i)} + \frac{v\,(t)}{L(\theta, i)} \tag{11}$$

the two variables can be defined as

$$a\,(t) = -\frac{R + \omega\partial L(\theta, i)/\partial\theta}{L(\theta, i)}$$

$$b\,(t) = \frac{1}{L(\theta, i)} \tag{12}$$

and (11) can be simplified as

$$\frac{di\,(t)}{dt} = a\,(t)\,i\,(t) + b\,(t)\,v\,(t) \tag{13}$$

It is assumed that the settling time of the current is much faster than the frequency of variations of the inductance. Furthermore, adaptive controller will be selected to operate much slower than the frequency of variations of the inductance due to the rotor position (i.e. rotor speed). Also, it is sufficient to develop the adaptive estimator only for one phase of the motor. To ensure stability of this model, estimation will be limited to periods where $a(t) < 0$. Then an observer model for the physical system can be assumed as

$$\frac{d\hat{i}\,(t)}{dt} = a_o\,(t)\,e\,(t) + \hat{a}\,(t)\,i\,(t) + \hat{b}\,(t)\,v\,(t) \tag{14}$$

where $e(t) = \hat{i}(t) - i(t)$ is the error of the estimation. $a_o(t)$ is the initial parameter of observer, $\hat{a}(t)$ and $\hat{b}(t)$ are parameters to be estimated. Since $a(t)$ and $b(t)$ are periodic functions based on the inductance profile of the machine, it is assumed that the variations from the model are only in the form of gains and so

$$a\,(t) = k_a a_m(t),\ \hat{a}\,(t) = \hat{k}_a a_m(t) \tag{15}$$

$$b\,(t) = k_b b_m(t),\ \hat{b}\,(t) = \hat{k}_b b_m(t) \tag{16}$$

where $\hat{k}_a$ and $\hat{k}_b$ are the parameters to be estimated while a_m and b_m are assumed to be known similar to the introduced parameters in (12). Then the observer model is rewritten as

$$\frac{d\hat{i}\,(t)}{dt} = a_m\,(t)\,e\,(t) + \hat{k}_a a_m\,(t)\,i\,(t) + \hat{k}_b b_m\,(t)\,v\,(t) \tag{17}$$

Hence, the error satisfies the differential equation

$$\frac{de\,(t)}{dt} = a_m(t)e(t) + (\hat{k}_a - k_a)a_m(t)i(t) + (\hat{k}_b - k_b)b_m(t)v(t) \tag{18}$$

and with adaptive law candidates

$$\frac{d\phi(t)}{dt} = \frac{d(\hat{k}_a a_m(t))}{dt} = -\gamma_1 a_m(t) e(t) i(t)$$
$$\frac{d\Psi(t)}{dt} = \frac{d(\hat{k}_b b_m(t))}{dt} = -\gamma_2 b_m(t) e(t) v(t) \tag{19}$$

The justification for the choice of the adaptive laws (19) is based on the Lyapunov function candidate [15]

$$V(e, \phi, \psi) = \frac{1}{2}[e^2(t) + \phi^2(t)/\gamma_1 + \psi^2(t)/\gamma_2] \tag{20}$$

$V(e, \phi, \psi)$ is a quadratic form and is positive-definite. Evaluating the derivative

$$\frac{dV}{dt} = a_m(t) e^2(t) < 0 \tag{21}$$

As it was mentioned before, $a_m(t)$ is periodic and is greater than zero for a portion of the period. However, that portion corresponds to the generating mode of DSSRM. This adaptive controller will be deactivated during phase angles corresponding to generation mode. Therefore, it can be guaranteed that this controller will only operate when $a_m(t) < 0$. Therefore, the adaptive observer is suspended during the generating conduction band. As a result, the adaptive law can be corrected as

$$\frac{d\phi}{dt} = -\gamma_1 a_m(t) e(t) i(t) w(t) \tag{22}$$
$$\frac{d\psi}{dt} = -\gamma_2 b_m(t) e(t) v(t) w(t) \tag{23}$$

where

$$w(t) = \begin{cases} 1 & a_m(t) < 0 \\ 0 & a_m(t) \geq 0 \end{cases} \tag{24}$$

hence, $dV/dt \leq 0$ and $V(e, \phi, \psi)$ is a Lyapunov function. For digital implement, above adaptive laws are transformed to discrete form

$$\phi(k) = \phi(k-1) - \gamma_1 T_m a_m(k) e(k) i(k) w(t) \tag{25}$$

$$\psi(k) = \psi(k-1) - \gamma_2 T_m b_m(k) e(k) v(k) w(t) \tag{26}$$

IV. RESULTS

In this section, we will validate the proposed method using various simulations and experimental analysis.

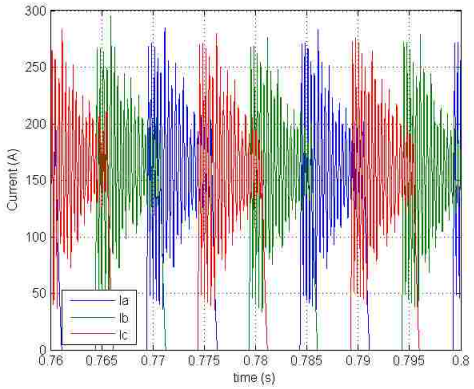

Fig. 5. Simulation results using a hysteresis current control.

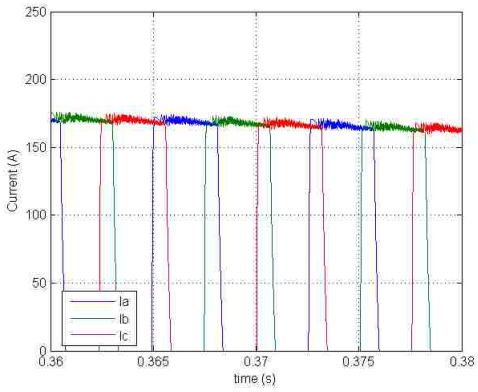

Fig. 6. Simulation results using the proposed MPC.

A. Simulation Results

In this section, it is assumed that a known reference current (i.e. I_{ref}) is an input to the current controller. The control block diagram is shown in Figure 4. This controller is simulated in the MATLAB for a DSSRM designed specifically for automotive applications. This motor has an inductance profile that is shown in Figure 2. The maximum input voltage and currents are 700 V, and 600 A respectively. Figure 5 illustrates the simulation results using a hysteresis current controller. It can be observed that the current ripple is unacceptable for a low audible noise, low torque ripple operation of the machine. This is due to very low phase inductances in combination with a high dc bus voltage. These conditions are required to achieve a wide speed ratio that is mandatory for automotive

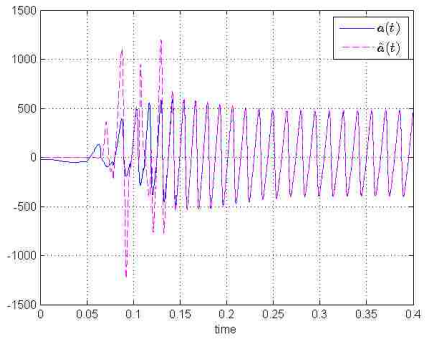

Fig. 7. Simulation results for estimation of a(t).

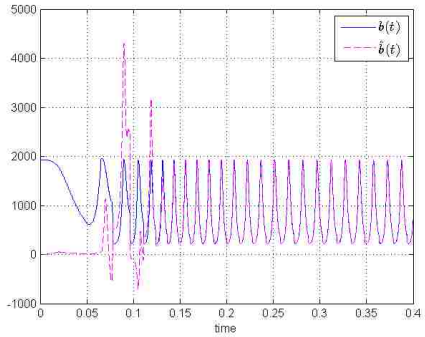

Fig. 8. Simulation results for estimation of b(t).

applications. Figure 6 demonstrates the performance improvement using the proposed MPC-based current controller. The reduced torque ripple will increase the efficiency, reduce the audible noise, and reduce the torque ripple of the DSSRM. Moreover, lower stresses over the DSSRM as well as the drive system introduces longer life-time for this automotive traction system.

Using an adaptive observer, the DSSRM dynamic parameters are identified and tracked as shown in Figure 7 and Figure 8, in which $\hat{a}(t)$ and $\hat{b}(t)$ is convergent to $a(t)$ and $b(t)$ respectively. In order to avoid unstable starting of system, it is recommended that the observer results are gradually implemented to predictive controller until the estimation error converges to zero within several cycles.

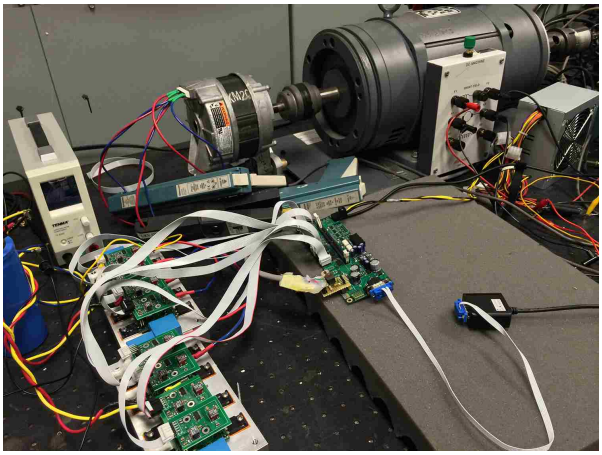

Fig. 9. The experimental test setup.

B. Experimental Results

the simulations were performed for a DSSRM for automotive applications, the experimental results are measured from a 0.5 HP 3-phase 12/8 SRM. This is due to a delay in manufacturing of the DSSRM. However, the results are promising and the proposed method can be applied to the DSSRM. In this test setup, the SRM is connected to a dc motor. Torque of the dc motor is controlled using the field current. This test setup is shown in Figure 9. The experimental results are measured from a drive system with a switching frequency of 1.5 kHz. Each phase of the motor is controlled with a different current control strategy to illustrate the effectiveness of MPC in comparison with the conventional methods. Results from this test are illustrated in Figure 10. Phase *a* of this motor is controlled using the proposed MPC with $N = 3$. Low current ripples are observed for this phase. Phase *b* is controlled using hard-chopping. It can be observed that the current ripple is much larger. Phase *c* is controlled using soft-chopping. Although the current of this phase is better than phase *b*, the ripples are higher than the ripples of phase *a*. Hence, model predictive current control of a switched reluctance machine can significantly improve the current ripple.

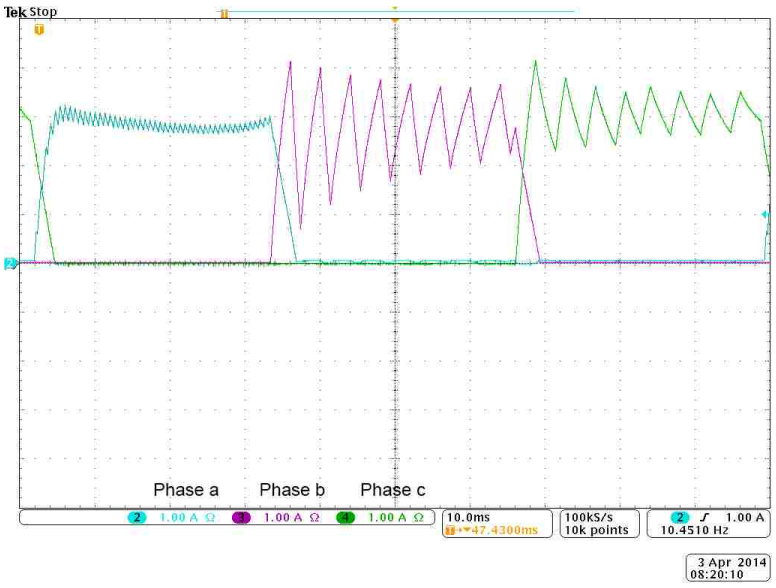

Fig. 10. Measured signals from a 3-phase SRM.

V. CONCLUSIONS

In this paper an adaptive model predictive control scheme was introduced. Due to a complete access to the model of the DSSRM, this paper implemented a model predictive control strategy for current control of the DSSRM using the exact inductance profile. In order to compensate for aging and inductance variations due to high temperatures and imperfect manufacturing, an adaptive observer was integrated with the MPC to follow the inductance variations of the machine. Simulation and experimental results demonstrated the performance improvement for this drive system. In conclusion, model predictive current control of a switched reluctance machine can significantly improve the current ripple while maintaining the high dynamics required during the activation and deactivation of each phase.

References

[1] C. Lin, W. Wang, and B. Fahimi, “Optimal design of double stator switched reluctance machine (dssrm),” in *Industrial Electronics (ISIE), 2012 IEEE International Symposium on*, 2012, pp. 719–724.

[2] M. Abbasian, B. Fahimi, and M. Moallem, "High torque double-stator switched reluctance machine for electric vehicle propulsion," in *Vehicle Power and Propulsion Conference (VPPC), 2010 IEEE*, 2010, pp. 1–5.

[3] G. Ramasamy, R. Rajandran, and N. Sahoo, "Modeling of switched reluctance motor drive system using matlab/simulink for performance analysis of current controllers," in *Power Electronics and Drives Systems, 2005. PEDS 2005. International Conference on*, vol. 2, 2005, pp. 892–897.

[4] P. Shamsi and B. Fahimi, "Single-bus star-connected switched reluctance drive," *Power Electronics, IEEE Transactions on*, vol. 28, no. 12, pp. 5578–5587, 2013.

[5] K. Rahman, B. Fahimi, G. Suresh, A. V. Rajarathnam, and M. Ehsani, "Advantages of switched reluctance motor applications to ev and hev: design and control issues," in *Industry Applications Conference, 1998. Thirty-Third IAS Annual Meeting. The 1998 IEEE*, vol. 1, 1998, pp. 327–334 vol.1.

[6] J. Chen, A. Prodic, R. Erickson, and D. Maksimovic, "Predictive digital current programmed control," *Power Electronics, IEEE Transactions on*, vol. 18, no. 1, pp. 411–419, 2003.

[7] H. Peyrl, G. Papafotiou, and M. Morari, "Model predictive torque control of a switched reluctance motor," in *Industrial Technology, 2009. ICIT 2009. IEEE International Conference on*, 2009, pp. 1–6.

[8] R. Mikail, I. Husain, Y. Sozer, M. Islam, and T. Sebastian, "A fixed switching frequency predictive current control method for switched reluctance machines," in *Energy Conversion Congress and Exposition (ECCE), 2012 IEEE*, 2012, pp. 843–847.

[9] J. Villegas, S. Vazquez, J. Carrasco, and I. Gil, "Model predictive control of a switched reluctance machine using discrete space vector modulation," in *Industrial Electronics (ISIE), 2010 IEEE International Symposium on*, 2010, pp. 3139 – 3144.

[10] L. Amor, O. Akhrif, L.-A. Dessaint, and G. Olivier, "Adaptive nonlinear torque control of a switched reluctance motor," in *American Control Conference, 1993*, 1993, pp. 2831–2836.

[11] A. Rahideh, M. Shaheed, and H. J. C. Huijberts, "Stable adaptive model predictive control for nonlinear systems," in *American Control Conference, 2008*, 2008, pp. 1673–1678.

[12] "Adaptive model predictive control for constrained nonlinear systems," *Systems & Control Letters*, vol. 58, no. 5, pp. 320 – 326, 2009.

[13] "Adaptive model predictive control for a class of constrained linear systems based on the comparison model," *Automatica*, vol. 43, no. 2, pp. 301 – 308, 2007.

[14] C. S. Edrington and B. Fahimi, "An auto-calibrating model for an 8/6 switched reluctance motor drive: application to design and control," in *Power Electronics Specialist Conference, 2003. PESC'03. 2003 IEEE 34th Annual*, vol. 1. IEEE, 2003, pp. 409–415.

[15] K. S. Narendra and A. M. Annaswamy, *Stable Adaptive Systems*. Dover Publications, Inc., 2005.

II. MODEL PREDICTIVE CURRENT CONTROL OF SWITCHED RELUCTANCE MOTORS WITH INDUCTANCE AUTO-CALIBRATION

Xin Li†, Student Member, IEEE, Pourya Shamsi††, Member, IEEE

Abstract

This paper investigates application of an unconstrained Model Predictive Controller (MPC) known as a finite horizon Linear Quadratic Regulator (LQR) for current control of a Switched Reluctance Motor (SRM). The proposed LQR can cope with the measurement noise as well as uncertainties within the machine inductance profile. Due to very low phase inductances of high-speed high-power SRMs, traditional delta modulation (fixed-frequency hysteresis) current controllers suffer from large ripples and are not suitable for such SRMs. Hence, application of MPC for Pulse Width Modulation (PWM) drive of these machines is of interest. In this paper, first a practical MPC scheme for embedded implementation of the system is introduced. Afterwards, Kalman filtering is used for state estimation while an adaptive controller is used to dynamically tune and update both MPC and Kalman models. Hence, the overall control structure is considered as a stochastic MPC with adaptive model calibration. Lastly, simulation and experimental results are provided to demonstrate the effectiveness of the proposed method.

Index Terms

SRM, MPC, Kalman filter, adaptive, predictive control, motor drive, current control.

† Xin Li is currently a graduate student at Missouri University of Science and Technology, Rolla, Missouri 65409 USA (email: xlg66@mst.edu).

†† Pourya Shamsi is currently with Missouri University of Science and Technology, Rolla, Missouri 65409 USA (email: shamsip@mst.edu).

I. INTRODUCTION

Conventionally, induction machines (IM) and permanent magnet motors (PM) are widely employed in electric vehicles (EV) [1] and air conditioning (HVAC) systems [2]. Some advantages of these machines in comparison with SRMs include simplicity of the drive and low acoustic noise. SRMs are mostly used for specialty applications including safety critical applications and high speed drives [3], [4]. Due to recent reductions in the cost of power electronics and superior properties of SRMs including rugged construction, low manufacturing costs, wide speed range, and high reliability, SRMs are becoming viable candidates for replacing IMs and PMs in variable speed drives [5]. In particular, double stator switched reluctance motor (DSSRM) has shown superior performance in power density which exceeds IM benchmarks while maintaining a low acoustic noise operation which makes this machine a candidate for the traction drive of future EVs [6].

SRMs operate based on complete switching of the magnetic field within each phase of the motor. Therefore, unlike IMs and PMs where the field variations correspond with a smooth sinusoidal functions, in SRMs, these variations occur in the form of a train of pulse. In order to provide the required sharp edges in this pulse train, a sufficiently large ratio between the dc bus voltage and the phase inductance is demanded. Maximum dc bus voltage is limited to the availability of a high voltage source as well as limitations induced by insulation classes and existing standards. Hence, in many practical applications, the phase inductance is used as a design parameter for controlling the maximum speed of the machine and maintaining the required pulse edge sharpness. Based on this introduction, it is expected to observe low phase inductances in high-power high-speed machines. Unfortunately, in high power applications, the maximum switching frequency of the semiconductor switches is limited by the switch technology. Hence, the drive system encounters a technical challenge in offering low phase current ripples for low inductance SRMs under limited switching frequencies.

Drive of SRMs has been a significant research topic with a variety of drive objectives such as position sensorless drives [7], [8], torque ripple reduction [9], and automotive drives with a wide speed range [10]. To ensure accurate tracking of the reference torque and current signals, an accurate current controller is of interest.

As a widely employed solution for SRMs, hysteresis controller (or bang-bang control) [11] has been effective in regulating the phase currents with a good dynamic response. However, this controller suffers from variable switching frequencies which leads to higher electromagnetic interferences. Also, ideal hysteresis control is not applicable as the maximum switching frequency is limited by the thermal response of the semiconductor technology. Hence, a practical hysteresis control has an upper cap for this frequency. Therefore, in many applications, this controller is implemented with the comparisons performed at fixed sample times and is known as a fixed frequency delta modulation. This approach will introduce high ripples in low inductance applications [12].

For this reason, research has been investigated to find alternative controllers with a fixed switching frequencies mostly by utilizing a PWM unit. A common approach for PWM current control is by incorporating a PI controller, however, as SRM winding inductance is inherently dependent on the phase current and rotor position, it is difficult to design PI parameters which well fit all operation conditions without any additional effort. Furthermore, a PI controller is not sufficiently fast to deliver sharp current pulse edges. Research for current control of SRMs include improved hysteresis control [13], improved PI control [14], [15], sliding mode control [11], model predictive control [16]–[18], and non-conventional methods such as neural networks [19]. Among these, MPC is a promising methods to handle the non-linear magnetic characteristic of SRMs, provide fast response, and maintain a fixed switching frequency.

MPC or receding horizon control offers good transient and fast tracking response. However, it has a high computational burden and requires accurate knowledge of the model. Various implementations of MPC have been reported in the power electronic literatures. Some common methods are Finite Control Set Model Predictive Control (FCS-MPC) [20] or Direct MPC [21]. FCS-MPC has gained a significant attention in the recent literatures on motor drives. Due to the finite number of possible circuit configurations in a power converter, it is possible to enumerate all feasible switching states for upcoming steps. Afterwards, by evaluating the cost function, the optimal control input is selected. FCS-MPC has low computational burden when predictive horizon is short. For motors with a neutral point and H-bridge drive topologies, methods like FCS-MPC perform well and provide a pattern similar to that of a PWM on each phase. However, this approach is

not applicable to SRMs. In SRMs, there are no significant interactions between different phases and hence, FCS-MPC suffers from current ripples as a fixed-frequency delta modulation.

Another approach is the single-step predictive control, or so-called the deadbeat control with PWM where the input vector is selected by solving the receding horizon problem for only a single step. This approach offers a straightforward closed-form expression and is easy to combine with other control strategies. However, a drawback of the deadbeat control is that it is sensitive to load variations, vulnerable to measurement noise, and cannot deliver multiple objectives. In addition to these common MPC methods, some other MPC approaches have been introduced in the literature such as the explicit MPC which is solved by multiple offline optimizations and is enforced using a lookup table [22], and the adaptive MPC which uses self-tuning techniques for model correction and calibration [23].

One of the main challenges in industrial deployment of a MPC current controller is the uncertainty of the model. The controller of a motor drive has feedbacks from current sensors such as resistor-based voltage sampling or Hall-effect transistors which contain a significant amount of noise and disturbances. These noises and disturbances often generated by electromagnetic interferences, zero drift, or gain drift and nonlinearities due to temperature variations [24]. In addition, a technical challenge in implementation of a MPC scheme for SRM is the inherent magnetic saturation during normal modes of operation. Unlike IMs, a SRM can have local magnetic saturations in currents below the nominal value. This effect is worsened in the +presence of eddy currents which are frequency dependent [25]. Hence, perturbations in the inductance profile of SRMs are a function of current, temperature, switching frequency, and rotor speed.

In this paper, a model predictive control with Kalman filtering and inductance profile auto-calibration is presented, which aims to address the introduced issues surrounding SRM current control. In particular, a tracking MPC is applied for current control and regulation in the machine. Kalman filters are used for state estimation by minimizing the influence of measurement noise. In addition, both MPC and Kalman filter parameters are updated dynamically using adaptive techniques to maintain an accurate model of the system. After analytical modeling, the proposed strategy is simulated. Lastly, experimental

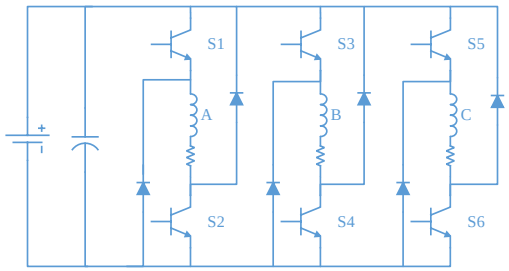

Fig. 1. The topology of an asymmetric bridge inverter.

results are provided to validate the proposed techniques.

II. MODEL PREDICTIVE CONTROL OF SRMS

Without loss of generality, a three phase 12/8 SRM is considered as the plant. However, the discussion results can be readily used in other SRMs as well. Figure 1 demonstrates the topology of a widely used asymmetric bridge for SRM drives. Unlike [26], in this topology, each phase of the SRM is controlled individually which eliminates any concerns regarding the deactivation of other phases. In this section, first two standard implementations of MPC in the form of LQRs are introduced, then a stochastic LQR is incorporated for SRM current control.

A. Dynamic Model of a SRM

In various SRM structures, the mutual inductance between adjacent phases are negligible. In order to derive a simple MPC scheme with low computational cost, the mutual inductance between phases are neglected. With this assumption, the flux linkage of a single phase of the machine is

$$\frac{d\psi\left(t\right)}{dt}=-R_s\frac{\psi\left(t\right)}{L\left(t,\psi\left(t\right),\theta\right)}+v\left(t\right) \tag{1}$$

where R_s is the phase resistance. To include saturation, $L(t,\psi(t),\theta)$ is the nonlinear position dependent inductance of each phase. $v(t)$ is the input voltage and the current can be calculated as $i(t)=\psi(t)/L(t,\psi(t),\theta)$. For a digital implementation, the SRM model is derived in the discrete-time domain using the forward method as

$$\psi_{k+1}=\left(1-T_s\frac{R_s}{L(k,\psi_k,\theta)}\right)\psi_k+T_sv_k \tag{2}$$

where T_s is the sampling time. In using the converter shown in Fig. 1, only one switch of each bridge is controlled using Pulse Width Modulation (PWM). For instance, during the operation of the phase a, S_1 is active while S_2 has a duty cycle of $d_k \in [0, 1]$. Therefore, each phase can generate a voltage in the set of $[0, V_{dc}]$. PWM control of the motor during the turn-off period is not required. During the turn-off period, the maximum negative voltage is generated by turning off both switches which corresponds to $-V_{dc}$. Hence, in (2), $v_k = d_k V_{dc}$. Also, since the control is much faster than the variations due to the rotor speed, it is assumed that $\bar{\theta}_k = \theta_k$ and $L(k, \psi_k, \bar{\theta}_k) \simeq L(k, \psi_k)$ which is simply denoted as L_k. This inductance is inherently periodic due to the mechanical structure of the machine. Depending on the number of rotor poles, the period will change. For standard machines, this period is often $\pi/4$ or $\pi/3$. Due to the periodic nature, the inductance of the machines can be represented using Fourier series such as [12]

$$L_k = l_0(i_k) + l_1(i_k)cos(4\bar{\theta}_k) + l_2(_k)cos(8\bar{\theta}_k) \tag{3}$$

where the Fourier coefficients $l_0(i_k)$ through $l_2(i_k)$ are calculated using

$$\begin{bmatrix} l_0(i_k) \\ l_1(i_k) \\ l_2(i_k) \end{bmatrix} = \begin{bmatrix} 0.25 & 0.5 & 0.25 \\ -0.5 & 0 & 0.5 \\ 0.25 & -0.5 & 0.25 \end{bmatrix} \begin{bmatrix} l_a(i_k) \\ l_m(i_k) \\ l_u(i_k) \end{bmatrix} \tag{4}$$

where $l_a(i_k)$, $l_m(i_k)$, and $l_u(i_k)$ are the inductance at fully aligned, midway, and unaligned positions of the rotor under phase current of i_k, respectively. Unfortunately, these parameters change during operation of the machine as a result of temperature variations and aging. Hence, a method for adaptive estimation of these parameters is proposed in the next section. An example plot of these parameters for the machine under study is depicted in Fig. 2.

Model of the SRM can be summarized as

$$\begin{cases} \psi_{k+1} = a_k \psi_k + b_k d_k \\ i_k = c_k \psi_k \end{cases} \tag{5}$$

where $a_k = 1 - T_s R_s / L_k$, $b_k = T_s V_{dc}$, and $c_k = 1/L_k$. This open-loop model is stable, reachable, and observable. Using the flux-linkage model in opposite to a current-based model avoids derivative of the inductance with respect to position and time which can lead to peaks due to noise and calculation error.

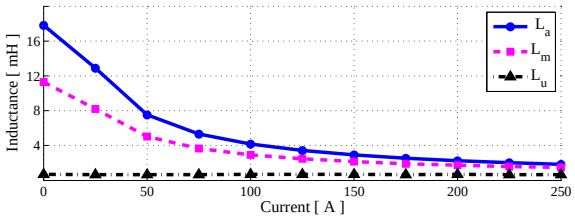

Fig. 2. Variations of the base inductance parameters as the function of phase current.

B. The Matrix Form of the Controller

MPC is a form of sub-optimal control which uses the model of the system to generate a sequence of future control actions for a finite prediction horizon under some constraints. MPC is often used in tracking applications. Also, a distinctive feature of MPC is the recalculation of the optimal input for each step of the control. Although the optimization includes multiple steps in the time horizon, only the immediate control input is used and future inputs are recalculated in upcoming sample times. In general, objectives are in the form of quadratic cost functions and constraints include the model of the system and boundaries on the input and states. To relax practical implementation of MPC, in this paper, mutual inductances were neglected. Hence, the model of SRM contains one linear differential equation and the objective function is in the form of a quadratic cost. Output of the MPC is the duty cycle for soft-chopping of the asymmetric bridge converter. Hence, the input has an inherent clamping function which limits it to the set of $[0, 1]$.

Since the goal of this paper is a practical implementation of the MPC, some assumptions are made. First, the objective function is selected as a sum of a quadratic function of the tracking error and a quadratic input cost function. Also, to reduce the computational burden, no additional input or state constraints are considered. It should be noted that a power converter has an inherent input constraint of $d \in [0, 1]$. However, if a proper input cost matrix is selected, the input will remain in this boundary and will only exceed this boundary when a large tracking command is exerted. For such scenarios, the input is clamped to the available boundary and is no longer optimal. However, in a practical application, this sub-optimality occurs in a small number of steps and is negligible. In return, the reduced complexity is of interest for practical deployment of the controller.

Elimination of any further constraints (other than the model itself) converts the MPC to a finite horizon LQR problem.

Traditionally, the matrix form of MPC was used as the control scheme. Examples include dynamic matrix control and a wide range of problems were solved using this approach [27]. Given a predictive horizon of H_p and a control horizon of $H_u \leq H_p$, the flux linkage model can be expressed as a known portion ψ_k and an unknown duty cycle vector $D_k = [d_{k|k}, \cdots, d_{k+H_u-1|k}]^T$. If the inductance variations are neglected for the time period of $t \in [kT_s, (k+H_p)T_s]$ (assuming a small sampling time, low mechanical speed, and a small predictive horizon), then the behavior of the system during the prediction horizon can be expressed as an augmented system of

$$\begin{bmatrix} \hat{\psi}_{k+1|k} \\ \vdots \\ \hat{\psi}_{k+H_u|k} \\ \vdots \\ \hat{\psi}_{k+H_p|k} \end{bmatrix} = \begin{bmatrix} a_k \\ \vdots \\ a_k^{H_u} \\ \vdots \\ a_k^{H_p} \end{bmatrix} \psi_k + \begin{bmatrix} b_k & 0 & \cdots & 0 \\ \vdots & \ddots & \ddots & \vdots \\ b_k a_k^{H_u-1} & b_k a_k^{H_u-2} & \cdots & b_k \\ \vdots & \vdots & \ddots & \vdots \\ b_k a_k^{H_p-1} & b_k a_k^{H_p-2} & \cdots & \sum_{j=0}^{H_p-H_u} b_k a_k^j \end{bmatrix} D_k \tag{6}$$

and the current is estimated as $[\hat{i}_{k+1|k}, \cdots, \hat{i}_{k+H_p|k}]^T = \mathbf{I}_{H_p} \otimes c_k [\hat{\psi}_{k+1|k}, \cdots, \hat{\psi} k + H_p|k]^T$ where $\mathbf{I}$ is the identity matrix and $\otimes$ is the Kronecker product. This augmented system can be modeled as $\hat{\Psi}_k = A_k \psi_k + B_k D_k$ and $\hat{I}_k = C_k \hat{\Psi}_k$. Additionally, the quadratic cost function considered is $J_{H_p|k} = (\hat{I}_k - I^*)^T Q (\hat{I}_k - I^*) + D_k^T R D_k$ where Q and R are the weight factors and I^* is the reference signal. In tracking applications, the input often has a non-zero mean. Hence, costing the input can reduce the accuracy of the control. Therefore, in some applications, $J_{H_p|k} = (\hat{I}_k - I^*)^T Q (\hat{I}_k - I^*) + \Delta D_k^T R \Delta D_k$ where $\Delta D_k = D_k - D_{k-1}$. In this paper, D_k is directly used for calculating the cost and observed results are satisfactory.

By substitution and expansion of the augmented model in the cost function, the cost function can be written as

$$J_{H_p|k} = D_k^T \left(B_k^T C_k^T Q C_k B_k + R \right) D_k + \delta_k^T Q \delta_k - 2\mathrm{Tr} \left(D_k^T B_k^T C_k^T Q \delta_k \right) \tag{7}$$

where $\delta = I^* - C_k A_k \psi_k$ is the tracking error. Since the problem is convex, the solution can be simply calculated by setting $\nabla_{D_k} J_{H_p|k} = 0$ as $2 \left(B_k^T C_k^T Q C_k B_k + R \right) D_k -$

$\mathrm{Tr}\left(2B_k^T C_k^T Q\delta_k\right) = 0$ and the optimal vector is

$$D_k = [B_k^T C_k^T Q C_k B_k + R]^{-1} B_k^T C_k^T Q[I^* - C_k A_k \psi_k] \tag{8}$$

and lastly, $d_{k|k}$ is applied to the system. This is equivalent to a single step recursive LQR on the augmented system. Although the derivation of the problem was simple and no dynamic programing was needed, the matrix inversion required for this input cannot be calculated easily.

If $R = 0$ and the horizon is set to unity, the algorithm is simplified and the MPC is transformed into the deadbeat control. In order to reduce the sensitivity of this deadbeat control, artificial sampling steps can be used (as introduced in [12]). In this approach, inputs are assumed to be constant over a number of m steps (or in the signal processing language, the actual sampling frequency is reduced by a ratio of m). If $m = H_p$, $d_{k|k} = (1-a_k)(I^* - c_k a_k^{H_p}\psi_k)/(b_k c_k(1-a_k Hp))$. The main purpose of this method is to minimize the required number of calculations while maintaining robustness to the noise.

C. Recursive Implementation of the Controller and Sub-optimal LQR

In practice and since the system has Markovian property, one can utilize standard dynamic programming to solve the problem backward in time. If the Markovian property does not hold, then the principal of optimality will not be met. In such conditions, one can often augment the state space to convert the system into a Markovian system. Examples of such systems include delayed control problems.

Results from this approach is similar to the original matrix form while the computational burden is reduced. Additionally, a simplified version is proposed for the SRM model. First, instead of augmenting the model and calculating the input vector as a single step LQR, the input can be calculated backward in time. Since the model of the SRM is scalar, this approach provides a simple solution ideal for practical implementations. In this approach, for the time period kT_s to $(k+H_p-1)T_s$ the inputs d_j for $j \in \{0,\cdots,H_p-1\}$ are calculated as

$$d_{k+j|k} = M_j[u_{j+1} - S_{j+1} a_k \psi_{k+j|k}] \tag{9}$$

$$M_j = [b_k^T S_{j+1} b_k + R]^{-1} b_k^T \tag{10}$$

$$S_j = c_k^T Q c_k + a_k^T S_{j+1}[I - b_k M_j S_{j+1}] a_k \tag{11}$$

$$u_j = a_k^T [I - b_k M_j S_{j+1}]^T u_{j+1} + c_k Q i^*_{k+j} \tag{12}$$

$$S_{H_p} = c_k^T Q c_k, \quad u_{H_p} = c_k^T Q i^*_{k+h_p} \tag{13}$$

where the sequences of M_j and S_j can be calculated for different angles and currents (for which the matrices a_k and c_k change) and stored in a table. These sequences can be re-calculated every time the inductance profile is updated. This approach requires more memory and in return, provides less computational burden. Two simplifications are possible in SRM drives.

II.C.1) Option 1: In SRM applications, the input reference needs not to vary during a control step as the firing angles can be adjusted to achieve the desired behavior. Variations of the reference will occur during the turn-off and turn-on periods. Therefore, instead of having a time varying sequence of i^*_j, the reference input can be constant during one control step and be updated for the next step. Using this simple approach, the u_j sequence can be calculated at a lower frequency (every time the inductance profile is updated) and only $d_{k|k}$ is calculated for every control step.

II.C.2) Option 2: In an additional level of sub-optimality, the tracking problem can be reduced to a settling problem. Define the error as $\varepsilon_{k+j|k} = i^*/c_k - \psi_{k+j|k}$ then $\varepsilon_{k+j+1|k} = a_k \varepsilon_{k+j|k} - b_k d_{k+j|k} - (1 - a_k) i^*/c_k$. Now, in a particular case of SRM applications, one can notice that $(1-a_k)/c_k = R_s T_s \simeq 0$. Then, the new model has only one input and can be studied as a settling LQR problem. Hence, the control sequence u_j is eliminated from (9)-(13) and the processing burden is reduced. Hence, $d_{k+j|k} = M_j S_{j+1} a_k (i^*/c_k - \psi_{k+j|k})$ where M_j and S_j are calculated as before. In practice, no significant difference between the performance of this simplification and the original LQR implementation is measurable.

D. Stochastic MPC and State-Estimation

A deterministic MPC was developed for SRMs in the prior section. In order to convert this MPC to a stochastic MPC both in model and inputs, further additions are required. In the first step, a Kalman estimator is developed to reduce the influence of stochastic sampling noise and improve the state estimation. In the next section, a system

identification approach will improve robustness of the proposed control to stochastic model variations.

Model of the SRM can be extended to include the stochastic noise as

$$\psi_{k+1} = a_k\psi_k + b_k d_k + g_k\mathcal{W}_k \tag{14}$$

$$i_k = c_k\psi_k + h_k\mathcal{M}_k \tag{15}$$

where $\mathcal{W}_k$ and $\mathcal{M}_k$ are zero-mean process and measurement noises, respectively. It should be noted that although this model is scalar, the following analytical studies are written in the general matrix form. Therefore, in that case of the matrix form, the gain matrices are written as G_g and H_k where $G_k = \bar{G}_k \otimes g_k$ and $\bar{G}_k = [G_{ij}]_k = a_k^{i-j} I_{i\geq j}$ where I_x is the indexer function ($I_x = 1$ if x is satisfied) and $H_k = \mathbf{I}_{H_p} \otimes h_k$ where $\mathbf{I}_{H_p}$ is an identity matrix of size H_p. Based on this model, the optimal input in (8) is no longer promising since ψ_k is a random variable and can contain the measurement noise. To ensure high performance operation of this controller, the expected value of the initial state should be used as $\mathsf{E}[\psi_k]$.

To mitigate the measurement noise, one can calculate the empirical mean using a large number of samples. However, this approach is not feasible for practical implementations. In this paper, a Kalman filter is incorporated to maintain an estimation of the mean of ψ_k. Using Kalman filter and assuming that the last measurement i_k is available and the noise process is a Wiener process, the flux can be corrected as

$$\psi_{k|k} = a_{k-1}\psi_{k-1|k-1} + b_{k-1}d_{k-1} + K_k[i_k - c_k(a_{k-1}\psi_{k-1|k-1} + b_{k-1}d_{k-1})] \tag{16}$$

where

$$K_k = P_k^- c_k^T[c_k P_k^- c_k^T + h_k\sigma_m^2 h_k^T]^{-1} \tag{17}$$

$$P_k^- = a_k P_{k-1} a_k^T + g_k\sigma_p^2 g_k^T \tag{18}$$

$$P_k = (\mathbf{I} - K_k c_k)P_k^- \tag{19}$$

which can be calculated easily for the model of this paper (it will be reduced to a set of scalar equations). Kalman parameters K_k and P_k are calculated recursively and will quickly converge to their steady state values. σ_m and σ_p are the measurement and process noise variances, respectively. In order to optimize the operation of Kalman filter,

these variances should be close to the physical values. To do so, one can utilize a separate estimator to calculate these parameters using empirical samples. Additionally, it is assumed that the added noise is zero-mean. Hence, Kalman filter cannot compensate for any drifts in the model. In the next section, drifts in the model are compensated using a separate inductance estimator.

III. INDUCTANCE AUTO-CALIBRATION

MPC will predict the behavior of the system and correct the optimal control input in every step to ensure fast and accurate dynamic response. However, a limited control horizon tends to increase the strength of each input. For this reason, in the first level, the ratio between Q and R matrices limits the excessive inputs by assigning a cost to the control input. In the second level, a Kalman filter is used to limit the influence of the noise on the prediction and the control input. However, it is still assumed that the model of the system is accurate. Otherwise, the prediction itself is no longer valid and each control output from the MPC guides the physical system to a different path than the reference tracking signal. Since MPC corrects the control signal in every step, this drift in the model is tolerable in many applications. However, in this paper, MPC is used mainly to reduce the current ripples by providing the optimal converter voltage based on the operation conditions of the machine. Hence, having an accurate model can significantly reduce the current ripples and provide the desired behavior. For this reason, on the third layer, a system identification approach is used to estimate the motor inductance and tune the control parameters for optimal performance.

Inductance variations in a SRM have fast and slow dynamical terms. Fast variations are caused by changes in the magnetic circuit as a result of rotor movement and changes in permeability as a result of saturation. These variations are deterministic. Therefore, the inductance can be represented as a function $l_k = L(\theta_k, i_k)$ where θ_k is the rotor position at time k and i is the phase current. The surface generated by this function in illustrated in Fig. 3. Slow variations of the inductance which correspond to slow variations of the function $L(.,.)$ are stochastic and are due to aging of bearings, deformations in the motor magnetic structure, and chemical reactions such as rusting as well as faults such as inter-turn short circuits within the windings. In this section, an inductor estimation

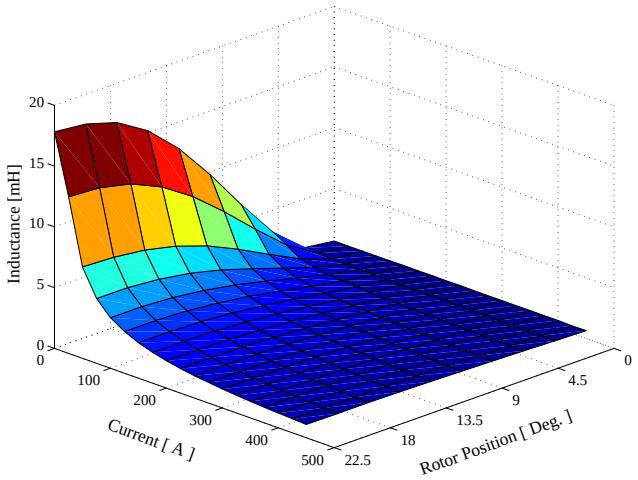

Fig. 3. Inductance profile of a 12/8 SRM as a function of rotor position and phase current.

and identification scheme is introduced to maintain a dynamic knowledge of the function $L(.,.)$. Using this function, optimal operation of the MPC is satisfied.

A discrete time adaptive estimation algorithm known as Recursive Least-Squares (RLS) is employed to estimate the inductance and eliminate the requirements for a matrix inversion of the standard Least-Squares Estimator (LSE). To perform the estimation, the inductance can be calculated directly using measured current samples. However, this approach requires derivation and is vulnerable to noise. For this reason, similar to the approach used in MPC, a flux model of the motor is used for derivation of the inductance profile. To do so, the flux is calculated by integration of the phase voltage. To eliminate drifts induced by the integration error, the flux is manually set to zero every time a phase has reached its firing angle. Therefore $\psi_k = T_s \sum_{n=1}^{n=k-1}(V_{dc}d_n - \hat{R}_s i_n) = \hat{l}_k i_k$ where $\hat{R}_s$ and $\hat{l}_k$ are the parameters to be estimated. It should be noted that the performance of this approach is highly influenced by parasitic parameters such as the voltage drop over the semiconductor switches. To cope with this problem, one can incorporate high frequency signal injection methods.

After acquiring a new estimate, the table (or discrete function) $L(\theta_k, i_k)$ is updated with the new estimate for $\hat{l}_k$. To do so, it is assumed that the shape of the inductance profile will not change. Hence, the inductance profile is still calculated using (3) and

(4). However, a gain coefficient is added to enforce the impacts of variations in the total inductance as $\hat{l}_k = \hat{\alpha}_k l_k = \hat{\alpha}_k L(\theta_k, i_k)$. Similarly, the resistance is estimated as $\hat{R}_s = \hat{\beta}_k R_s$. By defining the estimation error $e_k = i_k - \hat{i}_k$ where i_k is the measured signal (which is filtered for reduction in the sampling noise), then

$$\hat{\gamma}_{k+1} = \hat{\gamma}_k + G_k e_k \tag{20}$$

$$G_k = F_k \phi_k / (1 + \phi_k^T F_k \phi_k) \tag{21}$$

$$F_{k+1} = (\mathbf{I} - G_k \phi_k^T) F_k / \rho \tag{22}$$

where $\gamma_k = [\alpha_k, \beta_k]^T$. $\rho \in (0, 1)$ is a discount (or forgetting) factor which controls the trade-off between the speed of convergence and robustness to noise. F_k is a weight factor matrix which is calculating the inverse of the training sequence iteratively and $F_0 > 0$. $\mathbf{I} \in \mathbb{R}^{2\times 2}$ is the unity matrix. ϕ_k is the regression vector and contains the derivatives of the estimated output with respect to the estimation parameters as $\phi_k = [\partial\hat{\psi}_k/\partial\hat{\alpha}_k,\ \partial\hat{\psi}_k/\partial\hat{\beta}_k]^T$ or

$$\phi_k = [i_k L_k,\ T_s \sum_{n=1}^{k-1} i_n R_s]^T \tag{23}$$

Using this method, both inductance and resistance are calibrated on-line. In order to ensure stability, variations of γ_k is limited to a closed set containing unity. If R_s is small, then this term can be neglected and the estimator is reduced to a scalar form which improves computational burden. Since the current has to be filtered, it is better to perform this estimation only when the current has been kept constant for a few sampling steps. In another word, this estimation should be performed while the phase current is regulated at a certain reference value and during the active region of each SRM phase. This requirement is easily achieved due to the nature of a SRM drive.

Lastly, this estimator can dynamically tune the model parameters in the MPC and Kalman filter controllers. The overall block diagram of the proposed scheme is depicted in Fig. 4. It should be noted that this block is needed per each phase of the SRM. For instance, in the case of a three phase SRM, three sets of control blocks are needed to drive the machine.

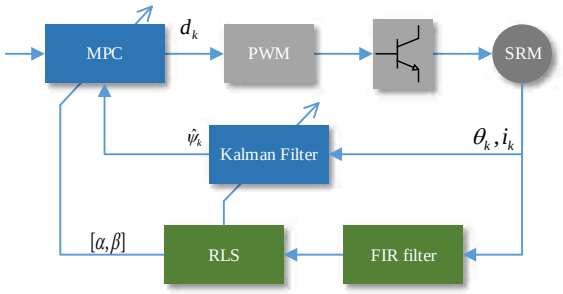

Fig. 4. Control block diagram of the overall system.

IV. SIMULATION RESULTS

In this section various simulations are provided to evaluate individual control blocks shown in Fig. 4.

A. Effectiveness of the Kalman Filter

In this scenario, the inductance estimator is deactivated and the MPC is studied with a fixed model. Also, performance behavior of the MPC with and without the Kalman filter is simulated and compared. For this purpose, a Gaussian noise is added to the simulation model and the behavior of the MPC is analyzed. In this scenario, two probability distribution functions are generated to represent the distribution of the current error. These functions are generated using the statistical data collected from the simulations. Fig. 5 illustrates the results from this study. It can be observed that the current tracking error is significantly reduced if the Kalman filter is present. It should be noted that not all variations are due to the noise. In SRM applications, due to the large amount of current ripples present, accurate estimation of the mean current is a technical challenge. Hence, even though the system is equipped with a Kalman filter and MPC, it cannot perfectly track the reference input signal and there will be ripples present in the measured signals.

B. Cost Function Analysis

In this scenario, 1000 Monte Carlo simulations of the system is performed to analyze the auto-calibration and Kalman filter. In each simulation, the value of the MPC cost

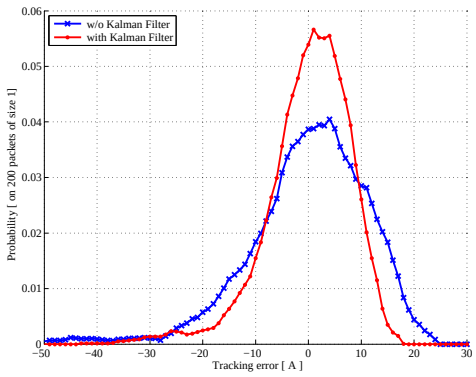

Fig. 5. Comparison between the distribution of two scenarios.

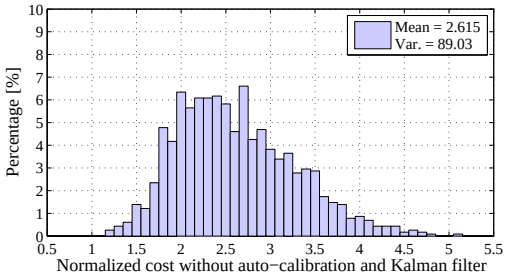

(a)

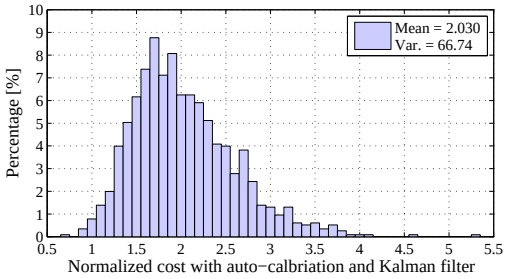

(b)

Fig. 6. Distributions of MPC objective function values, (a) without Kalman filter and auto-calibration, (b) with Kalman filter and auto-calibration.

function is stored. In the end, the distributions for the two scenarios are generated and are illustrated in Fig. 6a and Fig. 6b.

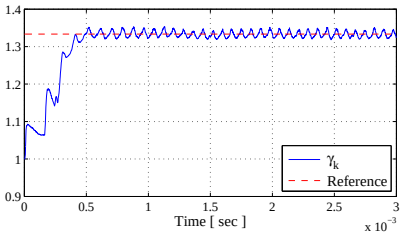

Fig. 7. Convergence of the RLSE.

C. Inductance Profile Adaptation

To validate the RLS inductance profile adaptation, the simulation is started with a wrong knowledge of profile which is at the 75 % of the actual inductance profile (25% lower than the motor parameters). Since the resistance is small, it is neglected and the RLS is reduced to the scalar form as aforementioned. It can be found in Fig. 7 that the RLS coefficient γ_k is convergent to around 1.33 which exactly compensates the difference between the pre-loaded and the actual inductance profiles (i.e. $0.75 \times 1.33 \simeq 1$). Consequently, the inductance profile is corrected by the RLS estimator for MPC and Kalman filter.

V. EXPERIMENTAL RESULTS

In this section, various experimental results are provided to evaluate the effectiveness of the proposed method. The experimental setup is developed using a three-phase 0.5 HP SRM, TI TMS320F28377D micro controller, and an asymmetric bridge inverter. In the first test, the motor is driven with a 20kHz delta modulation (fixed frequency hysteresis) controller and with a reference current of 3 A. During this test, motor is rotating at 100RPM which corresponds to low internally induced voltages and higher ripples. Current measurements for this scenario are illustrated in Fig. 8.

The same test is performed under the proposed simplified LQR control with a sampling frequency of 10kHz (to correspond with a 20kHz delta modulation if a switching event occurs in each comparison window). Results are illustrated in Fig. 9. It can be observed that the current ripples are much lower for the same reference current of 3 A and dc bus voltage of 60 V. Hence, LQR is a good control approach for SRM drives.

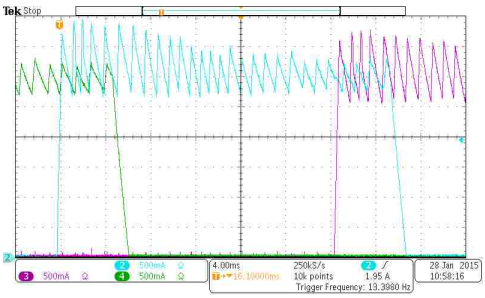

Fig. 8. Current ripples under a 20kHz sample time delta modulation.

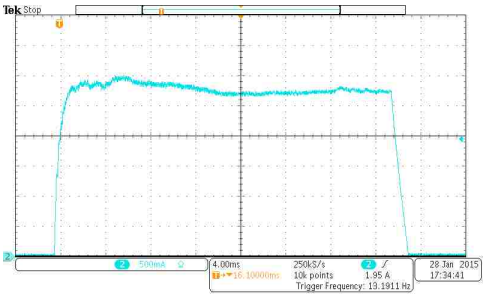

Fig. 9. Current ripples for the simplified LQR controller with no inductance profile adaptation.

In Fig. 9, one can notice a tracking error as a result of the mismatch between the model and the physical system. By enabling the inductance profile adaptation method proposed in this paper, this error is reduced as it is depicted in Fig. 10. The remaining mismatch in the shape of this signal is as the result of curve fitting errors in modeling the inductance surface using the Fourier and Taylor series with a low number of representative basis functions.

VI. CONCLUSIONS

In this paper, a model predictive current controller for applications in switched reluctance motor drives was introduced. This controller is equipped with Kalman filter state estimators. Additionally, to cope with model variations, two adaptive gains were dynamically calculated to compensate for the inductance and resistance mismatch between the model and the physical system. These adaptive estimators were implemented in

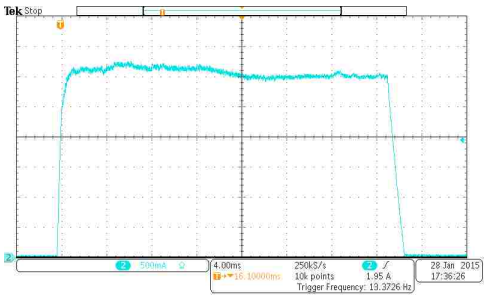

Fig. 10. Current ripples for the simplified LQR controller with inductance profile adaptation.

the form of a recursive least squares estimators. In conclusion, the proposed control scheme is successful in providing low current ripples and ensuring successful tracking of the reference current signal in SRM drives. Simulation and experimental results were provided to evaluate the effectiveness of the proposed controller.

References

[1] M. Ehsani, K. M. Rahman, and H. A. Toliyat, "Propulsion system design of electric and hybrid vehicles," *Industrial Electronics, IEEE Transactions on*, vol. 44, no. 1, pp. 19–27, 1997.

[2] M. Chomat and T. A. Lipo, "Adjustable-speed single-phase im drive with reduced number of switches," *Industry Applications, IEEE Transactions on*, vol. 39, no. 3, pp. 819–825, 2003.

[3] N. Matsui, T. Kosaka, N. Minoshima, and Y. Ohdachi, "Development of srm for spindle motor system," in *Industry Applications Conference, 1998. Thirty-Third IAS Annual Meeting. The 1998 IEEE*, vol. 1. IEEE, 1998, pp. 580–585.

[4] J. Han, X. Zhou, A. von Jouanne, A. Wallace, D. Marckx, and G. Hjelmeland, "Design of an srm-based actuator for high-performance steering vane control on the landing craft air cushion (lcac) hovercraft," in *Industry Applications Conference, 2004. 39th IAS Annual Meeting. Conference Record of the 2004 IEEE*, vol. 3. IEEE, 2004, pp. 1598–1601.

[5] K. M. Rahman, B. Fahimi, G. Suresh, A. V. Rajarathnam, and M. Ehsani, "Advantages of switched reluctance motor applications to ev and hev: design and control issues," *Industry Applications, IEEE Transactions on*, vol. 36, no. 1, pp. 111–121, 2000.

[6] C. Lin, W. Wang, and B. Fahimi, "Optimal design of double stator switched reluctance machine (dssrm)," in *Industrial Electronics (ISIE), 2012 IEEE International Symposium on*, May 2012, pp. 719–724.

[7] M. Ehsani, I. Husain, and A. B. Kulkarni, "Elimination of discrete position sensor and current sensor in switched reluctance motor drives," *Industry Applications, IEEE Transactions on*, vol. 28, no. 1, pp. 128–135, 1992.

[8] M. Ehsani and B. Fahimi, "Elimination of position sensors in switched reluctance motor drives: state of the art and future trends," *Industrial Electronics, IEEE Transactions on*, vol. 49, no. 1, pp. 40–47, 2002.

[9] B. Bilgin, A. Emadi, and M. Krishnamurthy, "Comprehensive evaluation of the dynamic performance of a 6/10 srm for traction application in phevs," *Industrial Electronics, IEEE Transactions on*, vol. 60, no. 7, pp. 2564–2575, 2013.

[10] M. Krishnamurthy, C. S. Edrington, A. Emadi, P. Asadi, M. Ehsani, and B. Fahimi, "Making the case for applications of switched reluctance motor technology in automotive products," *Power Electronics, IEEE Transactions on*, vol. 21, no. 3, pp. 659–675, 2006.

[11] S. M. Lukic and A. Emadi, "State-switching control technique for switched reluctance motor drives: Theory and implementation," *Industrial Electronics, IEEE Transactions on*, vol. 57, no. 9, pp. 2932–2938, 2010.

[12] X. Li and P. Shamsi, "Adaptive model predictive current control for dssrm drives," in *Transportation Electrification Conference and Expo (ITEC), 2014 IEEE*, June 2014, pp. 1–5.

[13] R. Gobbi and K. Ramar, "Optimisation techniques for a hysteresis current controller to minimise torque ripple in switched reluctance motors," *IET electric power applications*, vol. 3, no. 5, pp. 453–460, 2009.

[14] S. E. Schulz and K. M. Rahman, "High-performance digital pi current regulator for ev switched reluctance motor drives," *Industry Applications, IEEE Transactions on*, vol. 39, no. 4, pp. 1118–1126, 2003.

[15] F. Blaabjerg, P. C. Kjaer, P. O. Rasmussen, and C. Cossar, "Improved digital current control methods in switched reluctance motor drives," *Power Electronics, IEEE Transactions on*, vol. 14, no. 3, pp. 563–572, 1999.

[16] R. Mikail, I. Husain, Y. Sozer, M. Islam, and T. Sebastian, "A fixed switching frequency predictive current control method for switched reluctance machines," *Industry Applications, IEEE Transactions on*, vol. 50, no. 6, pp. 3717–3726, Nov 2014.

[17] T. Geyer, G. Papafotiou, and M. Morari, "Model predictive direct torque controlpart i: Concept, algorithm, and analysis," *Industrial Electronics, IEEE Transactions on*, vol. 56, no. 6, pp. 1894–1905, 2009.

[18] A. Linder, R. Kanchan, R. Kennel, and P. Stolze, *Model-based predictive control of electric drives*. Cuvillier, 2010.

[19] Z. Lin, D. Reay, B. Williams, and X. He, "High-performance current control for switched reluctance motors based on on-line estimated parameters," *IET electric power applications*, vol. 4, no. 1, pp. 67–74, 2010.

[20] S. Kouro, P. Cortés, R. Vargas, U. Ammann, and J. Rodríguez, "Model predictive controla simple and powerful method to control power converters," *Industrial Electronics, IEEE Transactions on*, vol. 56, no. 6, pp. 1826–1838, 2009.

[21] P. KaraMaNaKOS, T. Geyer, N. Oikonomou, F. Kieferndorf, and S. MaNIaS, "Direct model predictive control: A review of strategies that achieve long prediction intervals for power electronics," *Industrial Electronics Magazine, IEEE*, vol. 8, no. 1, pp. 32–43, 2014.

[22] A. G. Beccuti, S. Mariethoz, S. Cliquennois, S. Wang, and M. Morari, "Explicit model predictive control of dc–dc switched-mode power supplies with extended kalman filtering," *Industrial Electronics, IEEE Transactions on*, vol. 56, no. 6, pp. 1864–1874, 2009.

[23] C. S. Edrington, B. Fahimi, and M. Krishnamurthy, "An autocalibrating inductance model for switched reluctance motor drives," *Industrial Electronics, IEEE Transactions on*, vol. 54, no. 4, pp. 2165–2173, 2007.

[24] A. Patel and M. Ferdowsi, "Current sensing for automotive electronicsa survey," *Vehicular Technology, IEEE Transactions on*, vol. 58, no. 8, pp. 4108–4119, 2009.

[25] M. Krishnamurthy, D. Kaluvagunta, and B. Fahimi, "Effects of high frequency excitation on the behavior of a switched reluctance machine," in *Electric Machines and Drives, 2005 IEEE International Conference on*. IEEE, 2005, pp. 186–192.

[26] P. Shamsi and B. Fahimi, "Single-bus star-connected switched reluctance drive," *Power Electronics, IEEE Transactions on*, vol. 28, no. 12, pp. 5578–5587, Dec 2013.

[27] J. M. Maciejowski, *Predictive control: with constraints*. Pearson education, 2002.

III. INDUCTANCE SURFACE LEARNING FOR MODEL PREDICTIVE CURRENT CONTROL OF SWITCHED RELUCTANCE MOTORS

Xin Li†, Student Member, IEEE, Pourya Shamsi††, Member, IEEE

Abstract

In this paper, a stochastic Model Predictive Control (MPC) scheme for the current control of Switched Reluctance Motors (SRM) is introduced. This MPC is equipped with state estimators and is implemented as a recursive linear quadratic regulator for practical deployments in hybrid vehicle applications. Additionally, a learning mechanism is developed to dynamically adapt to the inductance profile of the machine and update the MPC and Kalman filter parameters. The introduced control scheme can cope with noise as well as uncertainties within the machine nonlinear inductance surface. The introduced system will benefit from a fixed switching frequency and will offer low current ripples by calculating the optimal duty cycles using the SRM model. Lastly simulations and experimental results are provided to evaluate the proposed method.

Index Terms

SRM, MPC, LQR, Kalman filter, inductance surface learning, predictive control, motor drive, switched reluctance, current control, delay compensation, inductance estimation.

† Xin Li is currently a graduate student at Missouri University of Science and Technology, Rolla, Missouri 65409 USA (email: xlg66@mst.edu).

†† Pourya Shamsi is currently with Missouri University of Science and Technology, Rolla, Missouri 65409 USA (email: shamsip@mst.edu).

I. INTRODUCTION

Recently, Switched Reluctance Motors (SRM) have gained more attention as alternatives to Induction Machines (IM) and Permanent Magnet Synchronous Machines (PMSM) in Hybrid Electric Vehicle (HEV) applications [1]–[3]. Also, SRMs have been utilized in HVAC systems, compressors, and many industrial applications where high speed high reliability machines are of interest [4]–[8]. In particular, due to the simple and rugged structure of these machines, their cost of manufacturing is relatively low and they have a very long life-span (in comparison with IMs and PMs). Simple rotor structure eliminates thermal management concerns regarding the rotor. Also, SRMs are able to operate at speed ratios of four to six (ratio between the top speed and the nominal speed) which is much higher than that of PMs. This feature has particularly encouraged electric vehicle manufacturers to consider SRMs as the traction machine [7].

Traditionally, SRMs were not considered as feasible industrial and commercial solutions for two main reasons. The first reason was the high amount of acoustic noise generated by these machines. This problem was mitigated by introduction of machines with lower acoustic noise such as the double stator SRMs [1]. The second challenge was the higher cost of the drive systems. SRMs require a high number of semiconductor switches in comparison with IM and PM drives. This problem has been recently mitigated by the significant reductions in the cost of semiconductor switches and introduction of new drive topologies such as [3]. Based on these solutions, there has been a growth on research and commercialization of low power switched reluctance machines.

Unfortunately, high power high speed SRMs which are used in HEV applications suffer from a third challenge that has to be addressed. Unlike rotational magnetic field machines, the reference current to each phase of SRM is a train of pulses. Hence, winding inductances should be sufficiently low to permit large variations of currents in short periods of time. In high power high speed SRMs, not only this time period is smaller, but also due to the higher power rating, the peak current is larger. Hence, these SRMs are designed with low phase inductances. It should be noted that in high speed motors, to cope with the internal induce voltage source of the machine, a large dc bus voltage is demanded as well. Therefore, there is a potential for high variations of the current if a

phase observes the dc bus voltage for a long period of time.

Meanwhile, high current semiconductor switches cannot operate at high frequencies. For many switch manufacturers, the maximum switching frequency of modules suitable for 50 to 500 HP drives is limited to 10 to 20 kHz. Hence, conventional hysteresis controllers require a constraint on the maximum switching frequency. Using such controllers, each phase of the SRM will observe one of the states of $+V_{dc}$, $-V_{dc}$, or 0 for at least 50 μs in a 20kHz operation which corresponds to large current ripples. For instance, in 2014, the U.S. department of energy invested in a 100 kW double stator SRM for applications in a hybrid truck. This SRM is capable of operating up to 10,000 RPM. To do so, this machine was designed for a dc bus voltage of 600 V and has a minimum inductance of 200 μH [2]. In low speeds where the internal voltage of the motor is negligible, the current ripple can be as high as 300 A for a 10 kHz switching frequency using a delta modulation control method. This amount is equivalent to 75% of the nominal current of the machine and can render the control of the machine ineffective. Hence, in this paper, a solution to this problem is offered using a Model Predictive Control (MPC) approach which will enable utilization of high speed high power SRMs in HEVs using low cost low frequency semiconductor switches.

Various papers have studied different current control techniques for SRM including conventional hysteresis control [9], PI controllers [10]–[12], MPC [13]–[15], sliding-mode methods [16], [17], and methods with integrated estimators [18]. In some applications similar to the one mentioned previously, fixed switching frequency hysteresis current controllers (i.e. delta modulation) are not suitable for SRM drive. The major drawback with this type of control is that the state of the switch cannot be changed faster than a preset time period which is dictated by the semiconductor limitations. Hence, the phase current can pass the hysteresis bands with no control. To cope with this problem, methods that can benefit from Pulse Width Modulations (PWM) are of interest. In such methods, the controller will generate a duty cycle that can mimic the internal voltage of the machine plus the additional voltage required to regulate the phase current. Hence, the regulation is achieved under a fix switching frequency with the ripples much lower than that of a delta modulation. A traditional approach to achieve this goal is by using a PI controller in combination with a PWM generator [19]. PI controllers have shown effectiveness in

variety of power electronics applications and are not model dependent. Although PIs have been used for SRM current control [10], [12], dynamics of these controllers are not fast enough to deliver sharp current edges. MPCs are highly dynamic and can be used to generate a reference duty cycle for the PWM unit [15], [20].

High dependency of the MPC to the model of the plant poses significant technical challenges in practical implementation of this type of control. In particular, model of SRM is both current and position dependent which leads to a set of nonlinear time-varying state equations. Additionally, this model will vary with aging and mechanical deformations. Hence, to utilize MPC for SRMs, not only the inductance as a function of current and rotor position is required, but also an estimation technique is needed to dynamically adapt to variations of this inductance surface. Some efforts are present in the literature to cope with variations of the model in SRM. For instance, iterative learning control was studied in [21]. In [20], the inductance profile as a function of current and rotor position was provided to the MPC. To cope with aging and further variations, adaptive estimators were incorporated to linearly gain the base inductance surface to match the new motor parameters. However, the main drawback with this approach is the inherent assumption that the Taylor and Fourier coefficients in representing the position and current dependency of the inductance surface remain unchanged. In practice, these values will change and the surface does not age linearly. For instance, rusting of the SRM magnetic core can reduce the aligned inductance. However, it has a negligible effect on the unaligned inductance of the machine. Hence, the shape of the inductance surface will change over time and a method to estimate the new nonlinear surface is of interest.

In this paper, a new model predictive current control of SRM is presented which benefits from state estimators using Kalman filters and a model identification unit based on an on-line inductance surface estimator. In this approach, the nonlinear inductance surface is locally linearized and the inductance data is recorded in a two dimensional table. This table is dynamically updated to maintain a knowledge of the true inductance surface of the machine. First, the principle and objective of a stochastic predictive current control for SRM is introduced in section II, and then various auto-calibration options are studies and evaluated in section III. Lastly, the proposed approach is simulated. Experimental results are provided to evaluate the control scheme.

II. MODEL PREDICTIVE CURRENT CONTROL OF SRMS

A. Model Formulation and Control

The model of a SRM can be derived based on variations of the current or variations of the flux. Current based models are good for electrical analysis of the machine. However, utilization of such models for MPC applications tend to generate inferior results compared to a flux-based model. This is mainly due to the term corresponding to the derivative of the motor inductance. In a current-based model, the derivative of the inductance profile is used which is not completely known in a SRM with stochastic variations of the model. For instance, if the inductance surface is generated using a table, the derivative of the inductance will have a lattice form with no useful information. In this paper, a flux-based model is used to form the MPC as

$$\begin{cases} \dot{\psi}_t = -R_s\psi_t/L_t + v_t + k_1\mathcal{W}_t \\ i_t = \psi_t/L_t + k_2\mathcal{M}_t \end{cases} \tag{1}$$

where $\psi(t)$ is the flux linkage of a phase of a machine and v_t is the input terminal voltage of the machine. In this model, mutual coupling between different phases of the machine are neglected (details regarding modeling the mutual flux is available in [22], [23]). R_s and $L(t)$ are the phase resistance and the phase inductance, respectively. $\mathcal{W}_t$ and $\mathcal{M}_t$ are standard Wiener processes to model process and measurement noise, respectively. k_1 and k_2 are used to tune the variances of the Wiener processes. This model is transformed into a discrete form using a forward method for digital implementation of the MPC as $\psi_{k+1} = a_k\psi_k + b_k d_k + k_1\mathcal{W}_k$ and $i_k = c_k\psi_k + k_2\mathcal{M}_k$ where $a_k = (1 - R_sT_s/L_k)$, $b_k = T_sV_{dc}$, and $c_k = 1/L_k$ where T_s is the sampling period, v_{dc} is the dc bus voltage, and d_k is the duty cycle of the converter for this period.

Another advantage of using a flux-based model is the coefficient a_k which is always within the unit circle (assuming that a proper T_s is selected). However, in a current-based model, this parameter is outside of the unit circle during the generation mode of operation.

For now, it is assumed that the model parameters are deterministic. Variations of the model parameters are studied in the next section. It should be emphasized that $L_k = L(\theta_k, i_k)$ is a function of the current itself. Hence, for now, it is assumed that during

the control step k, i_k which is the measurement at time k is available and the controller can use this parameter to derive the parameter L_k. Later, a new method is introduced to compensate for the delays if i_k is not available.

MPC or receding horizon control is an attractive control technique for many motor drive applications [24]. In many motor drive applications, the objective function is in the form of a quadratic cost and no further constraints other than the model itself is present. In this case, the problem is known as a finite horizon Least Quadratic Regulator (LQR) and can be solved using

$$d_{k+j|k} = M_j[u_{j+1} - S_{j+1}a_k\psi_{k+j|k}] \tag{2}$$

$$M_j = [b_k^T S_{j+1} b_k + R]^{-1} b_k^T \tag{3}$$

$$S_j = c_k^T Q c_k + a_k^T S_{j+1}[I - b_k M_j S_{j+1}]a_k \tag{4}$$

$$u_j = a_k^T[I - b_k M_j S_{j+1}]^T u_{j+1} + c_k Q i^*_{k+j} \tag{5}$$

$$S_{H_p} = c_k^T Q c_k, \quad u_{H_p} = c_k^T Q i^*_{k+h_p} \tag{6}$$

where Q and R are the tracking and input cost matrices, respectively. P is the length of the control horizon and $j \in \{0, \cdots, P-1\}$. i^*_{k+j} is the tracking reference signal.

To reduce the effect of the noise on $\psi_{k+j|k}$, Kalman filtering can be incorporated. For this purpose, if i_k is available,

$$\begin{aligned}\psi_{k|k} &= a_{k-1}\psi_{k-1|k-1} + b_{k-1}d_{k-1} \\ &\quad + K_k[i_k - c_k(a_{k-1}\psi_{k-1|k-1} + b_{k-1}d_{k-1})]\end{aligned} \tag{7}$$

where

$$K_k = P_k^- c_k^T[c_k P_k^- c_k^T + h_k h_k^T]^{-1} \tag{8}$$

$$P_k^- = a_k P_{k-1} a_k^T + g_k g_k^T \tag{9}$$

$$P_k = (\mathbf{I} - K_k c_k) P_k^- \tag{10}$$

and hence the controller is capable of driving the motor under stochastic measurement and process noise.

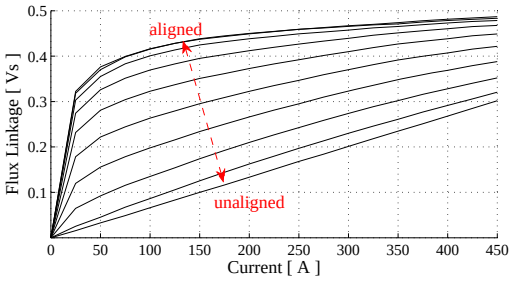

Fig. 1. Flux linkage within a SRM.

B. Delay Compensation

If there exists a delay between the measurement of i_k and the control step k, then the previous Kalman filter needs to be modified. Such delays occur in many practical applications if low cost low speed analog to digital converters are utilized or if multiple samples are used to generate a low noise signal using a finite impulse response filter. In this case, the most recent information is at time $k-1$ which is i_{k-1}. Hence, $\psi_{k|k-1}$ can be calculated as

$$\begin{aligned}\psi_{k|k-1} &= a_{k-1}\psi_{k-1|k-2} + b_{k-1}d_{k-1} \\ &\quad + a_{k-1}K_{k-1}[i_{k-1} - c_{k-1}\psi_{k-1|k-2}]\end{aligned} \tag{11}$$

and K_{k-1} is calculated as before. Now, the controller has an expected knowledge of ψ_k based on information state in $k-1$. The next step is to get an information regarding the duo $\hat{i}_k$ and $\hat{L}_k$ based on the fact that $\psi_{k|k-1} = \hat{i}_{k|k-1}\hat{L}_k$ and using a prior knowledge on the magnetics characteristics of the core.

Flux linkage of the SRM as a function of the current is shown in Fig. 1. Based on the rotor position, the flux linkage curve has to follow a path set by the magnetic characteristics of the material. Therefore, by using the last two sets of observations, the expected value of $\hat{i}_k$ can be estimated using a gradient descent method as

$$\hat{i}_k(0) = i_{k-2}, \quad \hat{i}_k(1) = i_{k-1} \tag{12}$$

$$\hat{L}_k(0) = L_{k-2}, \quad \hat{L}_k(1) = L_{k-1} \tag{13}$$

$$\hat{\psi}_k(j) = \hat{i}_k(j)\hat{L}_k(j) \tag{14}$$

$$\hat{i}_k(j+1) = \hat{i}_k(j) + (\psi_{k|k-1} - \hat{\psi}_k(j)) \times (\hat{i}_k(j) - \hat{i}_k(j-1))/(\psi_{k|k-1} - \hat{\psi}_k(j)) \quad (15)$$

$$\hat{L}_k(j+1) = L(\theta_{k-1|k-1}, \hat{i}_k(j+1)) \quad (16)$$

where (14)-(16) are calculated repeatedly until $|\hat{\psi}_k(j) - \psi_{k|k-1}| < \varepsilon$ which is the convergence criterion. Although this approach works satisfactory during normal modes of operation of the SRM or in systems with no inductance surface learning, if large model variations occur, this approach will not converge to the correct value. Later, it is shown that if the starting inductance model is not accurate enough or if a significant deformation occurs, the learning mechanism will start to adapt to the new model based on the newly observed information. However, this information does not arrive simultaneously and the inductance model will converge slowly. Hence, there will be times that the flux linkage model is not monotonically increasing and local minima will appear. Under such circumstances, a gradient descent approach is no longer satisfactory and will get stuck in local minima (unless i_k, i_{k-1}, and i_{k-2} are close enough). For such scenarios, heuristic search algorithms such as multi-tribal differential evolution or multi-agent stair case (hill climbing) can be used. The goal is to find every minimum of the function, hence, if a minimum is found, the function in the vicinity of that minimum should be unreachable to other agents. After finding every minimum and assuming that a proper control sampling time was selected, the minimum closest to the location of i_{k-1} is the solution since the current cannot have large deviations during one T_s period.

III. INDUCTANCE SURFACE LEARNING

A lookup table is a simple method to describe the nonlinear inductance surface of the SRM. Lookup tables for torque, flux linkage and inductances of SRMs are widely used in past [25], [26]. In particular, due to the nonlinear nature of the inductance surface in SRMs, estimating and maintaining the knowledge of this inductance profile is of interest [27], [28]. MPC is a highly model dependent method and without an accurate knowledge of the inductance surface, this method can lead to large control errors [29].

Several methods have been proposed for inductance profile auto-calibration or learning [30]–[32]. One options is to use analytical equations; the model parameters are updated

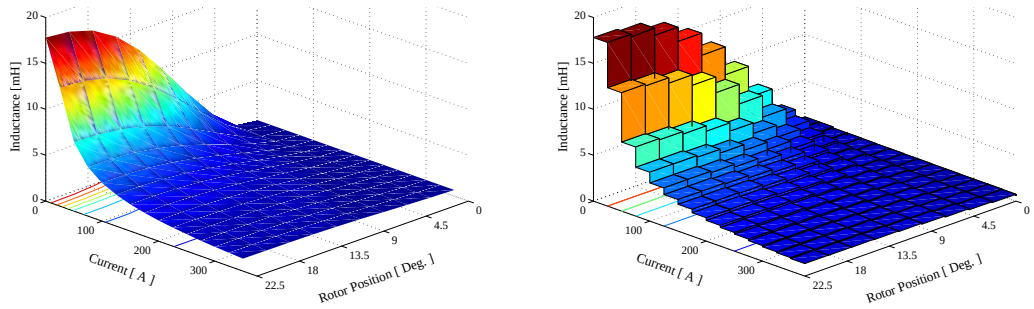

(a) (b)

Fig. 2. Inductance surface of SRM, (a) the actual surface, (b) a quantized surface to be stored in the table.

directly and recursively by calculating the controller or observer errors. Due to the presence of noise in a practical application, it is not easy to tune the auto-calibration algorithm and to balance the trade-off between the convergence speed and accuracy. Therefore, it is better to have a separate estimator and not use the main controller to update the estimation (which can lead to instability of the controller as well). Also, using analytical models such as Taylor and Fourier series (for instance, in [20]) requires extensive amount of information to tune the high number of coefficients used. This problem is a multi-input multi-output regression problem and requires an extensive amount of matrix operations and inversions. On the other hand, the table-based auto-calibration is a more stable solution which does not demand a high computational burden as the table entries are updated individually in a piecemeal manner. The calibration of each element of table is only driven by the corresponding current and rotor position rather than the entire operation range feedbacks. The main drawback of this method is the larger memory requirements. However, cost of fast processors is higher than memory modules and therefore, table based approach is more appealing to industrial and commercial deployments.

A table containing the knowledge of the inductance surface can be generated by quantizing the original inductance surface calculated using finite elements analysis of the SRM. Quantization resolution will control the trade-off between the memory requirements and accuracy. Fig. 2a illustrates the inductance surface of a 12/8 SRM. To quantize this surface, a set of currents and a set of angles are selected to form a two dimensional

grid. The inductance at each node of this grid is recorded in the matrix to form a quantized inductance surface. The quantized surface of Fig. 2a is illustrated in Fig. 2b. The procedure of lookup table auto-calibration can be briefly summarized as three steps. In the first step, the inductance is generated from the lookup table for the MPC. In the second step, a new inductance value is estimated from prior flux linkage and current estimations for a local current-rotor position region. lastly, the table is updated with the new inductance estimation in a filtered manner.

A. Inductance Estimation

A well-known method for on-line inductance profile identification is to inject a high frequency current into the phase winding and measure the induced voltage amplitude. However, for high power inverters, it is impossible to inject high frequency currents as the maximum frequency of switches is limited by the semiconductor technology. A solution to this problem is to utilize separate high frequency signal injection mechanisms. Another approach is to use the flux linkage of the machine.

In SRMs, since the flux linkage and current go to zero periodically, the phase flux linkage may be obtained from the integral of the phase voltages [28].

$$\hat{\psi}_k = \psi_0 + T_s \sum_{j=1}^{k-1} (V_{dc} d_j - R_s i_j) \tag{17}$$

Normally it is assumed that $\psi_0 = 0$ at the beginning of each firing period. A benefit of using the flux is the integration of the measured signals which acts as a low pass filter to dampen the zero mean noise of measurements. For further reduction of the measurement noise, signals can be filtered using finite impulse response filters such as a moving average filter prior to this integration. The new inductance estimate can be derived as $\hat{L}(\theta_k, i_k) = \hat{\psi}_k / i_k$ where θ_k is the position of the motor at the moment of this calculation. However, this integration is highly influenced by parasitic circuit elements such as switch and wire voltage drops.

Using any desired method, a new inductance estimate is acquired which will be used to update the table using a procedure introduced later.

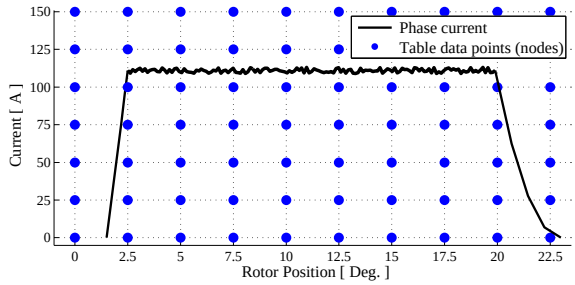

(a)

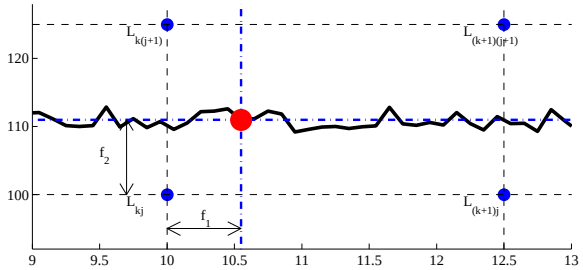

(b)

Fig. 3. Flow of the desired current-position point on the quantized inductance table, (a) a current sample path with respect to the table, (b) f_1 and f_2 parameters with respect to the desired current-position point and table nodes.

B. Table Usage Protocol

Before introducing the update procedure, a protocol for using the inductance table is introduced. A quantized inductance table is shown in Fig. 3a. In this figure, a sample current path for one phase of the SRM is shown. Also, a grid of quantized current-rotor angle nodes are observable which are the locations for individual table entries. To use the quantized inductance table, one can simply use the data stored in the table entry located at the nearest current-position node. However, to benefit from a linear interpolation, the data is retrieved as

$$L(\theta, i) = \phi^{(\theta,i)} \beta^{(\theta,i)} \tag{18}$$

where $\phi^{(\theta,i)} = [(1-f_1)(1-f_2), (1-f_1)f_2, f_1(1-f_2), f_1 f_2]$ defines the location of the desired measurement with respect to the quantized information where $f_1 \in [0, 1)$ and $f_2 \in [0, 1)$ are the angle and current distances between the desired value and the nearest

quantized nodes, respectively. These parameters are calculated as $f_1 = (\theta - \lfloor\theta\rfloor_{\theta_{stp}})/\theta_{stp}$ and $f_2 = (i - \lfloor i\rfloor_{i_{stp}})/i_{stp}$ where i_{stp} and θ_{stp} are the quantization resolutions for current and angle, respectively. $\lfloor j\rfloor_q$ calculates the lower quantized value of j with respect to the step-size j_{stp}. Implementing this function is very easy on any type of digital controllers. These parameters are illustrated in Fig. 3b for a sample point of interest of with a current of 111 A and rotor position of 10.5 degrees.

$\beta^{(\theta,i)} = [L_{kj}, L_{k(j+1)}, L_{(k+1)j}, L_{(k+1)(j+1)}]$ contains the information of the nodes surrounding the desired point of (θ, i) where k is the index of $\lfloor\theta\rfloor_{\theta_{stp}}$ and j is the index of $\lfloor i\rfloor_{i_{stp}}$. Using this approach, all four entries surrounding an observation point can be updated with suitable influence ratios defined by the distances f_1 and f_2. This approach will not only improve the accuracy of data interpolation, but also will improve the convergence performance of the learning mechanism introduced in the following part.

C. Recursive Least-Square Estimation

A discrete time adaptive estimation algorithm known as Recursive Least-Squares (RLS) is employed to gradually learn the inductance table and eliminate the requirements for a matrix inversion of the standard least-squares method. To perform the estimation, updates to the four surrounding nodes derived above can be performed in a learning fashion as

$$\beta_{k+1}^{(\theta,i)} = \beta_k^{(\theta,i)} + G_k(\hat{L}(\theta_k, i_k) - \phi_k^{(\theta,i)}\beta_k^{(\theta,i)}) \tag{19}$$

where $G_k = F_k[\phi_k^{(\theta,i)}]^T/(1 + \phi_k^{(\theta,i)}F_k[\phi_k^{(\theta,i)}]^T)$ and $F_{k+1} = (I - G_k\phi_k^{(\theta,i)})F_k/\rho$ is the weighting matrix where $\rho \in (0, 1)$ defines the learning rate. F_0 is a positive definite diagonal matrix. Using this method, β for each rectangular location will converge to a steady state value which corresponds to the convergence of each table entry.

The overall schematic of the proposed inductance table and learning mechanism is shown in Fig. 4a and the overall control scheme is shown in Fig. 4b. This scheme is per phase of a SRM. Hence, a three phase SRM requires three parallel control mechanisms. In order to reduce the computational and memory burden, one can assume that different phases of a machine perform similarly, therefore, the inductance table can be shared between different phases.

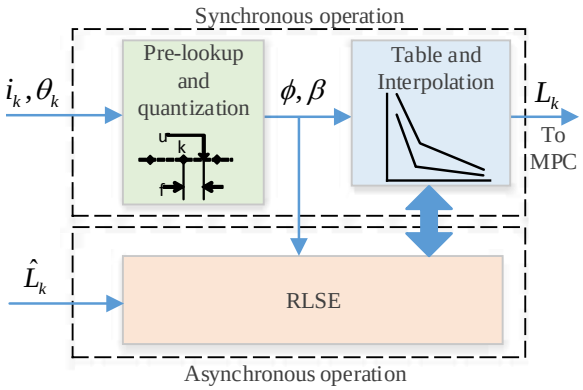

(a)

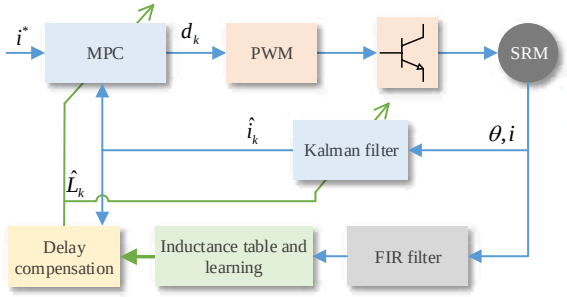

(b)

Fig. 4. Control diagrams, (a) inductance table and learning mechanism, (b) the overall control scheme.

IV. SIMULATION RESULTS

A. Delay Compensation

In this scenario, the effectiveness of a delay compensator block for the MPC is simulated and studied. A Simulink model is generated for a SRM controlled with the block diagrams shown in Fig. 4. This model has a control and modulation frequency of 10 kHz and the simulation step is set to 1 μs. The delay compensator is deactivated for one phase of this machine. Results comparing the performance of the MPC for these two scenarios are shown in Fig. 5. It can be observed that the phase with a delay compensator performs significantly better than the case with no compensation.

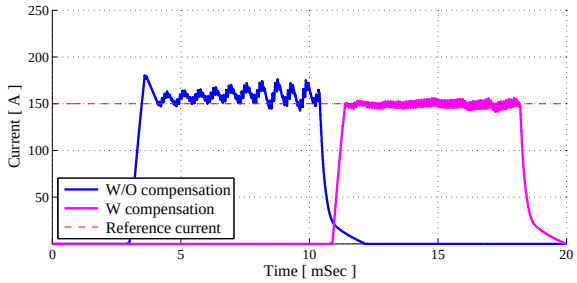

Fig. 5. Effectiveness of the delay compensator.

B. Inductance Surface Learning

Although the inductance surface is shown beforehand for a computer based simulation, in this scenario, the simulation is started with a wrong knowledge of the inductance profile. This inductance table is shown in Fig. 6a. In order to increase the visibility of the figure, the inverse of the inductance profile is shown. Hence, the contour value are in fact $(1\ \mathrm{mH})/\mathrm{L_k}$.

In the first step, a reference current of 150 A is selected. Using this reference, the model is simulated for a period of time. During this period, a phase of the machine was activated several times and rotor positions ranging within $[0, 22.5]$ were observed multiple times. In each observation, the new estimate of the inductance was gradually transfered to the inductance table using (19). Fig. 6b illustrates these data points and the new inductance table values.

In the next step, the reference is increase to 250 A and data is plotted in Fig. 6c. It can be observed from this figure that the region of 150 A from Fig. 6a and Fig. 6b are significantly different and the table has learned the inductance profile corresponding to 150 A. Additionally, it can be observed from Fig. 6c that the system has learned the new profile corresponding to the current of 250 A as well. These figures illustrate the effectives of the proposed algorithm in identifying and learning the true model of the machine on-line.

In particular, phase current of the SRM for the first four cycles after setting the reference of 150 A is shown in Fig. 7. It can be observed that the first cycle of operating at this references has much higher inaccuracies and ripples compared to the fourth cycle.

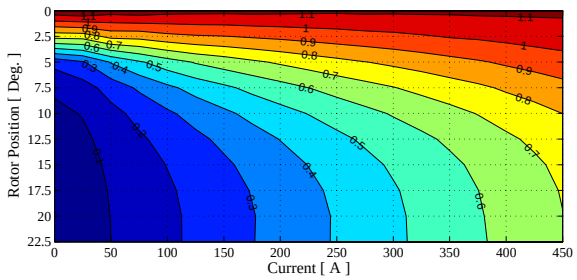

(a)

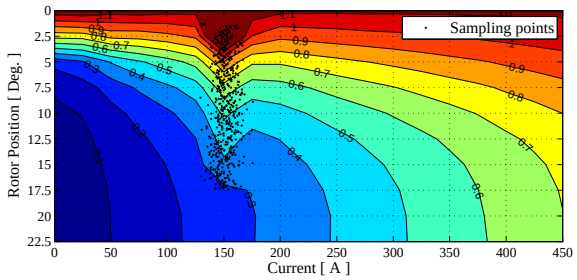

(b)

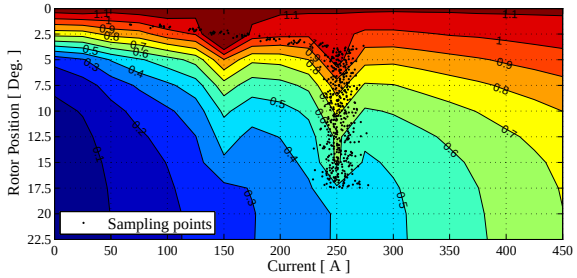

(c)

Fig. 6. Inductance learning simulation, (a) loaded table, (b) learning for 150 A, (c) learning for 250 A.

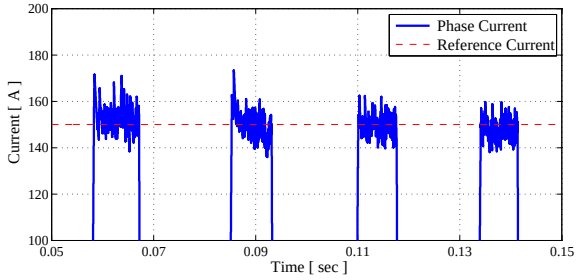

Fig. 7. Learning the inductance profile over four cycles.

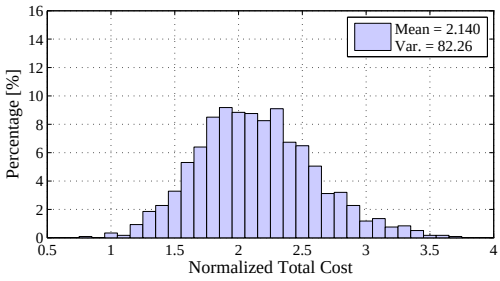

(a)

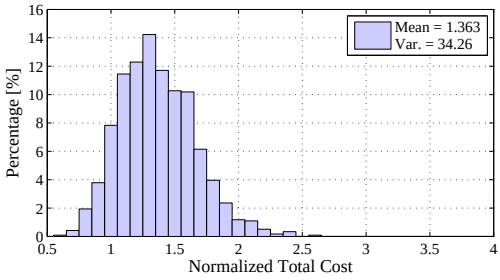

(b)

Fig. 8. Distributions of MPC objective function values, (a) without learning mechanism, (b) with learning mechanism.

In fact, the mean value of the current during this cycle is higher than the reference of 150 A. This is due to the inaccurate model loaded to the simulation. However, after only four cycles of operation, the learning mechanism has identified and updated the correct inductance profile into the table. Therefore, during the fourth cycle, MPC is performing much better than the first cycle which is visually noticeable. It should be noted that the loaded data is only 25 % higher than the actual inductance surface. In practice, this difference might be higher and the system cannot operate accurately without a learning mechanism.

C. Inductance Learning and Improved MPC

In this section the cost function of the MPC is studied with and without the introduced inductance learning mechanism. For this reason, 1000 Monte Carlo simulations of the system is performed with and without the learning mechanism. In each simulation, the value of the MPC objective function is stored. In the end, distribution functions for the

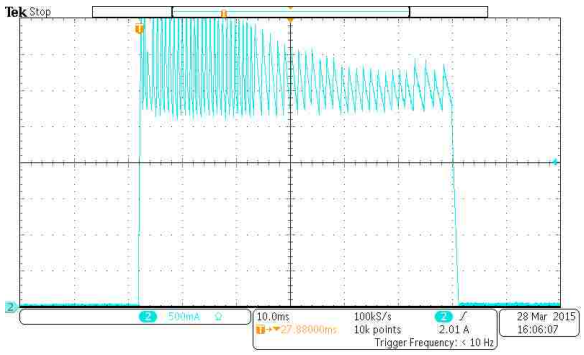

Fig. 9. Delta modulation at a fixed sampling rate of 20kHz.

two scenarios are generated and are illustrated in Fig. 8a and Fig. 8b. Based on these figures, it is observed that the mean and deviations of the cost function is lower for the case with a learning mechanism. This cost corresponds to a better tracking and MPC performance.

V. EXPERIMENTAL RESULTS

In this section, experimental tests and measurements are provided to demonstrate the effectiveness of the proposed algorithms. In the first test, a delta modulation current control of a three phase SRM at a reference current of 3 A and a speed of 50 RPM is studied. Current measurements for this test are illustrated in Fig. 9. Based on this figure, one can observe that a delta modulation approach is not effective in regulating the current of this machine. Hence, a MPC for generating the reference duty cycles for a PWM control of the machine is of interest.

Fig. 10 illustrates the implementation of the proposed recursive LQR current controller with the same reference current and at the same speed. In this scenario, the inductance table is directly utilized by selecting the closest inductance entry based on the angle and phase currents. Hence, no interpolation is used for this scenario. It can be observed that large tracking deviations occur at positions where the controller is switching between different table entries.

To cope with this problem, Fig. 11 illustrates the same test when the proposed linear table interpolation mechanism is used. It can be observed that the tracking performance

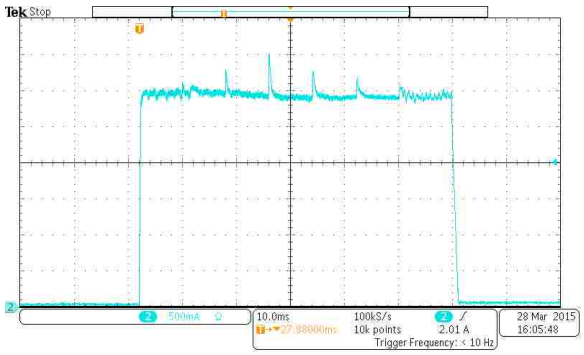

Fig. 10. Recursive LQR current control at a sampling rate of 10kHz with no inductance table interpolation.

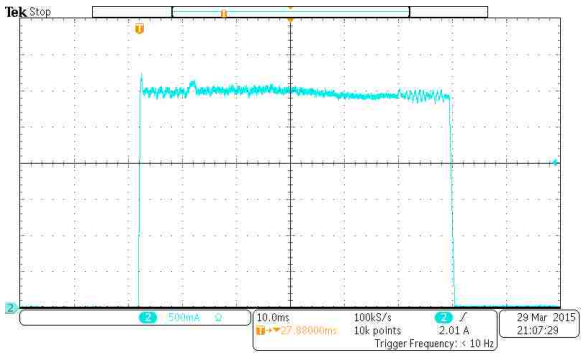

Fig. 11. Recursive LQR current control with inductance table interpolation.

is significantly improved with the interpolation mechanism in place.

In the next case study, the speed is increased to 250 RPM. At higher speeds, the magnitude of the internal induced voltage of the motor is increased. This voltage is highly dependent on the inductance surface of the machine. To demonstrate the demand for the proposed learning mechanism, in the first test, the learning mechanism is deactivated. Hence, the control scheme suffers from a mismatch between the utilized model and the physical system. Fig. 12 illustrates the measured current control results at this speed. It can be observed that there is a significant tracking error when the internal induced voltage is at its maximum.

In Fig. 13, the inductance surface learning and delay compensation mechanisms are both activated. It can be observed that the performance of the LQR current controller

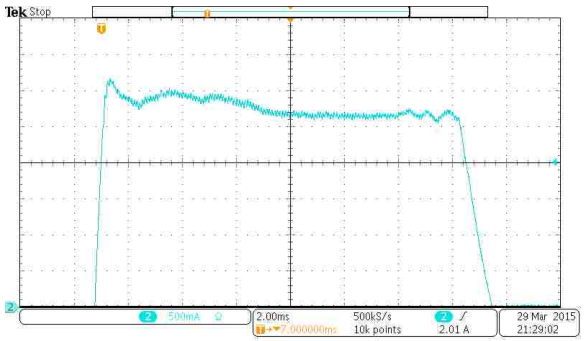

Fig. 12. LQR with no inductance surface learning or delay compensation.

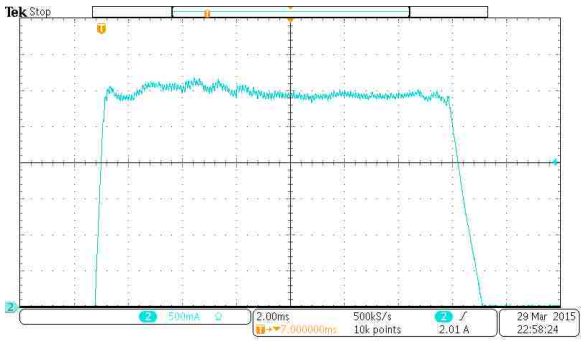

Fig. 13. LQR with inductance surface learning and delay compensation.

is improved significantly. These results demonstrate the effectiveness of the proposed techniques in current control of a SRM.

VI. CONCLUSION

This paper was focused on a mechanism to learn and adapt to the inductance surface of a switched reluctance motor to perform a model predictive current control of this machine. This inductance surface was stored in the form of a table to be used with a model predictive current controller with Kalman state estimators. The learning mechanism is utilizing a recursive least squares estimator to update individual entries in the SRM inductance table. Additionally, an interpolation mechanism was introduced to improve the accuracy of the reconstructed inductance surface using the quantized inductance table. Also, a delay compensation technique was introduced to cope with measurement delays

in MPC of a SRM. Simulation results and experimental measurements were provided to demonstrate the effectiveness of the proposed inductance surface learning mechanism in increasing the performance of model predictive current control of a SRM.

References

[1] C. Lin, W. Wang, and B. Fahimi, "Optimal design of double stator switched reluctance machine (dssrm)," in *Industrial Electronics (ISIE), 2012 IEEE International Symposium on*, May 2012, pp. 719–724.

[2] "Double-stator switched reluctance motor technology," REACT, Department of Energy, Advanced Research Projects Agency - Energy (ARPA-E), 2012, [Report]. [Online]. Available: http://arpa-e.energy.gov/?q=slick-sheet-project/double-stator-motor-design

[3] P. Shamsi and B. Fahimi, "Single-bus star-connected switched reluctance drive," *Power Electronics, IEEE Transactions on*, vol. 28, no. 12, pp. 5578–5587, 2013.

[4] M. Ehsani, K. M. Rahman, and H. A. Toliyat, "Propulsion system design of electric and hybrid vehicles," *Industrial Electronics, IEEE Transactions on*, vol. 44, no. 1, pp. 19–27, 1997.

[5] F. Abrahamsen, F. Blaabjerg, J. K. Pedersen, P. Z. Grabowski, and P. Thogersen, "On the energy optimized control of standard and high-efficiency induction motors in ct and hvac applications," *Industry Applications, IEEE Transactions on*, vol. 34, no. 4, pp. 822–831, 1998.

[6] K. Kiyota and A. Chiba, "Design of switched reluctance motor competitive to 60-kw ipmsm in third-generation hybrid electric vehicle," *Industry Applications, IEEE Transactions on*, vol. 48, no. 6, pp. 2303–2309, 2012.

[7] M. Krishnamurthy, C. S. Edrington, A. Emadi, P. Asadi, M. Ehsani, and B. Fahimi, "Making the case for applications of switched reluctance motor technology in automotive products," *Power Electronics, IEEE Transactions on*, vol. 21, no. 3, pp. 659–675, 2006.

[8] Y. Yang, N. Schofield, and A. Emadi, "Double-rotor switched reluctance machine (drsrm)."

[9] R. Gobbi and K. Ramar, "Optimisation techniques for a hysteresis current controller to minimise torque ripple in switched reluctance motors," *IET electric power applications*, vol. 3, no. 5, pp. 453–460, 2009.

[10] S. E. Schulz and K. M. Rahman, "High-performance digital pi current regulator for ev switched reluctance motor drives," *Industry Applications, IEEE Transactions on*, vol. 39, no. 4, pp. 1118–1126, 2003.

[11] F. Blaabjerg, P. C. Kjaer, P. O. Rasmussen, and C. Cossar, "Improved digital current control methods in switched reluctance motor drives," *Power Electronics, IEEE Transactions on*, vol. 14, no. 3, pp. 563–572, 1999.

[12] B. Shao and A. Emadi, "A digital pwm control for switched reluctance motor drives," in *Vehicle Power and Propulsion Conference (VPPC), 2010 IEEE*, Sept 2010, pp. 1–6.

[13] Y.-R. Mohamed and E. F. El-Saadany, "Robust high bandwidth discrete-time predictive current control with predictive internal modela unified approach for voltage-source pwm converters," *Power Electronics, IEEE Transactions on*, vol. 23, no. 1, pp. 126–136, 2008.

[14] S. Kouro, P. Cortés, R. Vargas, U. Ammann, and J. Rodríguez, "Model predictive controla simple and powerful method to control power converters," *Industrial Electronics, IEEE Transactions on*, vol. 56, no. 6, pp. 1826–1838, 2009.

[15] R. Mikail, I. Husain, Y. Sozer, M. Islam, and T. Sebastian, "A fixed switching frequency predictive current control method for switched reluctance machines," *Industry Applications, IEEE Transactions on*, vol. 50, no. 6, pp. 3717–3726, 2014.

[16] S. M. Lukic and A. Emadi, "State-switching control technique for switched reluctance motor drives: Theory and implementation," *Industrial Electronics, IEEE Transactions on*, vol. 57, no. 9, pp. 2932–2938, 2010.

[17] J. Ye, P. Malysz, and A. Emadi, "A fixed-switching-frequency integral sliding mode current controller for switched reluctance motor drives," 2014.

[18] Z. Lin, D. Reay, B. Williams, and X. He, "High-performance current control for switched reluctance motors based on on-line estimated parameters," *IET electric power applications*, vol. 4, no. 1, pp. 67–74, 2010.

[19] F. Peng and A. Emadi, "A digital pwm current controller for switched reluctance motor drives," in *Transportation Electrification Conference and Expo (ITEC), 2014 IEEE*. IEEE, 2014, pp. 1–6.

[20] X. Li and P. Shamsi, "Adaptive model predictive current control for dssrm drives," in *Transportation Electrification Conference and Expo (ITEC), 2014 IEEE*. IEEE, 2014, pp. 1–5.

[21] C. Lai, Y. Zheng, A. Labak, and N. C. Kar, "Investigation and analysis of iterative learning-based current control algorithm for switched reluctance motor applications," in *Electrical Machines (ICEM), 2014 International Conference on*. IEEE, 2014, pp. 796–802.

[22] J. Ye, B. Bilgin, and A. Emadi, "Elimination of mutual flux effect on rotor position estimation of switched reluctance motor drives considering magnetic saturation," *Power Electronics, IEEE Transactions on*, vol. 30, no. 2, pp. 532–536, 2015.

[23] ——, "Elimination of mutual flux effect on rotor position estimation of switched reluctance motor drives," 2015.

[24] J. Rodriguez and P. Cortes, *Predictive control of power converters and electrical drives*. John Wiley & Sons, 2012, vol. 40.

[25] H. Hannoun, M. Hilairet, and C. Marchand, "Design of an srm speed control strategy for a wide range of operating speeds," *Industrial Electronics, IEEE Transactions on*, vol. 57, no. 9, pp. 2911–2921, 2010.

[26] G. Gallegos-Lopez, P. C. Kjaer, and T. Miller, "High-grade position estimation for srm drives using flux linkage/current correction model," *Industry Applications, IEEE Transactions on*, vol. 35, no. 4, pp. 859–869, 1999.

[27] P. Chancharoensook and M. F. Rahman, "Dynamic modeling of a four-phase 8/6 switched reluctance motor using current and torque look-up tables," in *IECON 02 [Industrial Electronics Society, IEEE 2002 28th Annual Conference of the]*, vol. 1. IEEE, 2002, pp. 491–496.

[28] R. A. McCann, M. S. Islam, and I. Husain, "Application of a sliding-mode observer for position and speed estimation in switched reluctance motor drives," *Industry Applications, IEEE Transactions on*, vol. 37, no. 1, pp. 51–58, 2001.

[29] J. Rodríguez, J. Pontt, C. A. Silva, P. Correa, P. Lezana, P. Cortés, and U. Ammann, "Predictive current control of a voltage source inverter," *Industrial Electronics, IEEE Transactions on*, vol. 54, no. 1, pp. 495–503, 2007.

[30] C. S. Edrington, B. Fahimi, and M. Krishnamurthy, "An autocalibrating inductance model for switched reluctance motor drives," *Industrial Electronics, IEEE Transactions on*, vol. 54, no. 4, pp. 2165–2173, 2007.

[31] P. Tandon, A. Rajarathnam, and M. Ehsani, "Self-tuning control of a switched-reluctance motor drive with shaft position sensor," *Industry Applications, IEEE Transactions on*, vol. 33, no. 4, pp. 1002–1010, 1997.

[32] S. Mir, I. Husain, and M. E. Elbuluk, "Switched reluctance motor modeling with on-line parameter identification," *Industry Applications, IEEE Transactions on*, vol. 34, no. 4, pp. 776–783, 1998.

SECTION

2. CONCLUSIONS

This thesis proposes three papers for model predictive current control of SRM. The first paper introduces a improved deadbeat MPC with adaptive estimator for deterministic system. If the measurement noise and uncertainty present, the second paper proposes a novel MPC current controller for SRM allowing for better decision making. The proposed controller composes of several modules for different functions, including long range MPC which determines optimal duty cycle for PWM, the Kalman filter for reducing the variance of processing and measuring noise, and the RLS with moving average for parameters auto-calibration. The functional parts and entire system are verified by Monte Carlo simulation, which proves that proposed method is feasible and has better performance in statistic terms. One of challenges which are not expanded in this paper is that the parameters tuning for MPC, Kalman filter and RLS themselves, however, relative discussions can be found in a large number of academic works of past decades. The novel MPC current controller for SRM proposed in third paper can cope with low inductance SRM which is not suitable for conventional hysteresis type current controller. When current measurement noises present, this method can reduce current tracking deviations in statistic terms by applying Kalman filter.. Furthermore, this method

allows user to guess reasonable parameters and calibrate them during operation when accurate inductances are not available due to measurement difficulties for high power SRM. The auto-calibration is table-based as the lookup can well fit the nonlinearity of SRM, meanwhile, the table-base updating is in piecemeal manner to prevent time-varying parameters in adaptive analytical equations which will be influenced in entire operation range.

VITA

Xin Li received the B.S. and M.S. degrees in Electrical Engineering from Tianjin University, Tianjin, China, in 2005 and 2007, respectively. He earned his M.S. degree in Electrical Engineering from Missouri University of Science and Technology in May 2015.

Xin Li was employed as a graduate research assistant at the Missouri University of Science and Technology under Dr. Pourya Shamsi from 2013 to 2015. Xin Li worked as a motor design engineer at Emerson Climate Technologies Ltd., Suzhou, China, from 2008 to 2013.